POLYTECHNICA UNIVERSITY OF BUCHAREST
FACULTY OF MATERIALS SCIENCE AND ENGEENERING

PhD THESIS

Research on the efficient use of critical raw materials as dopants in zirconium-based materials for extreme applications

Scientific coordinators:

Prof. Dr. Eng. Cristian PREDESCU

Author:

Anca Elena SLOBOZEANU

President	***Prof.univ.dr.eng. Brandușa GHIBAN*** *Politechnica University of Bucharest*
Scientific coordinators	***Prof.univ.dr.eng. Cristian PREDESCU*** *Politechnica University of Bucharest*
Scientific referees	***Prof.univ.dr.eng. Alina Adriana MINEA*** *Technical University Gheorghe Asachi Iasi* ***CSI,dr.ing. Roxana Mioara PITICESCU*** *I.N.C.D.M.N.R Pantelimon* ***Prof.univ.dr.chem. Ecaterina MATEI*** *Politechnica University of Bucharest*

Bucharest

2023

Summary

LIST OF ACRONYMS

UE - European Union

CRM - Critical Raw Materials

REE – Rare earth elements

REO – rare earth oxides

TBC - thermal barrier coatings

HREE - Heavy rare earth elements

LREE - Light rare earth elements

PGM - Platinum group metals

LCO - Lithium cobalt oxide

NCA - Nickel-cobalt-aluminum oxide

NMC - nickel oxide, manganese, cobalt

TEC - Coefficients of thermal expansion

RZO - Rare earth zirconates

Keywords: critical raw materials, rare earths, hydrothermal synthesis, rare earth doped zirconia, thermal barriers.

INTRODUCTION

The growing interest in the production of a wide range of goods and services used in everyday life, the development of new materials, advanced components necessary to support important applications, but also an increase in the population and the fact that the resources of our earth are limited, raising the issue of the supply of raw materials in the future. The increase in global demand for metals and minerals is due to the acceleration of innovation, industrialization, digitization and the rapid growth of emerging economies, which are especially necessary for the development of new technologies that are more efficient in terms of eco-efficiency and competitiveness. All these technologies are closely related to the great challenges of society, which are mobility, climate change, health and the need for new concepts of urban development. Therefore, raw materials, forming a strong industrial base, are crucial to the global economy. Ensuring access to a stable market for raw materials has become a major challenge especially for regional and national economies with limited production, such as the economy of the European Union (EU), which relies on imports of many metals and minerals needed for industry, including many critical raw materials [1–3].

The European Commission launched the European Raw Materials Initiative in 2008, an integrated strategy addressing the ongoing concern to secure and improve access to raw materials for the EU. The establishment of a list of critical raw materials (CRM) at European level, reviewed periodically (every 3 years) was one of the priority actions of this Initiative [1]. This list also includes rare earth elements (REEs), elements that play a critical role in the global economy.

The motivation for choosing the research theme came from the identified problem regarding the complexity of the separation process in individual rare earth oxides (REO). This fact is due to their similar electronic configuration and physico-chemical properties and is reflected in high-priced products with a large environmental footprint. In recent years, there has been an increasing interest in the use of various REO mixtures as dopants for high-temperature ceramics, especially for ZrO_2-based thermal barrier coatings (TBCs) used in aeronautics and cogeneration. The use of mixed REO can increase the working temperature of TBCs due to the formation of tetragonal and cubic solid solutions with higher melting temperatures, avoiding grain thickening due to interface segregation, enhancing its ionic conductivity and sinterability. The thermal stability of the coatings can be further improved by using rare earth zirconates with perovskite or pyrochlore structures that do not have phase transitions before melting.

Through the research carried out in the doctoral thesis, the effective use of CRMs, more precisely rare earth elements, as dopants in ZrO_2-based materials for potential applications in the field of thermal barriers was pursued.

Therefore, the objective of the thesis is to demonstrate the potential of using mixtures of rare earth oxides (mixture that simulates the natural composition of monazite concentrates), as dopants in the design of zirconia-based coatings, which contribute to an efficient use of critical raw materials, with an impact on ensuring the transition to climate neutrality.

Thus, the elimination of separation steps and the use of mixed REOs instead of individual REOs can bring about an important decrease in production costs along the entire manufacturing cycle, from raw materials to product. At the same time, an important aspect of the doctoral thesis is the development of advanced nanomaterials for high-tech applications for thermal barriers. Thus, the elimination of separation steps and the use of mixed REOs instead of individual REOs can bring about an important decrease in production costs along the entire manufacturing cycle, from raw materials to product. At the same time, an important aspect of the doctoral thesis is the development of advanced nanomaterials for high-tech applications for thermal barriers.

Thus, the elimination of separation steps and the use of mixed REOs instead of individual REOs can bring about an important decrease in production costs along the entire manufacturing cycle, from raw materials to product. At the same time, an important aspect of the doctoral thesis is the development of advanced nanomaterials for high-tech applications for thermal barriers [2].

The doctoral thesis is structured in two parts:

☑ **general part,** represented by **chapters I and II,** which includes the current state of knowledge, in which the analysis of specialized literature in the field of the research theme is presented;

☑ **original part,** developed in chapters **III, IV, V, VI,** which includes the sum of the experimental results and own contributions in the field addressed. The experimental part is focused on two research directions, and a market study, namely: research on the development of ceramic powders based on ZrO_2 doped with a synthetic mixture of rare earths; research on the development of thermal barriers based on ZrO_2 ceramic materials doped with a synthetic mixture of rare earths, market research on thermal barriers.

Chapter I, entitled **"THE CURRENT STATE REGARDING CRITICAL MATERIALS AND THEIR ROLE IN GREEN ENERGY. RARE EARTHS AS CRITICAL MATERIALS",** presents a synthetic analysis from current specialized literature, regarding the criticality of raw materials and their role in strategic technologies, with an emphasis on rare earth elements - types of ores, production and their applications.

Chapter II, entitled **THE CURRENT STATE OF RESEARCH IN THE FIELD OF THERMAL BARRIERS BASED ON ZrO2 DOPED WITH RARE EARTHS,** is dedicated both to obtaining ceramic materials based on ZrO_2 doped with rare earths and to obtaining thermal barriers based on ZrO_2 doped with rare earths. Thus, a theoretical foundation is presented regarding the structure of ZrO_2, but also information regarding the doping of zirconia with rare earths. At the same time, recent information regarding the synesis methods and the deposition processes approached for the development of these types of materials are presented. The most relevant results obtained in this field are briefly presented.

Chapter III, RESEARCH OBJECTIVES AND METHODOLOGY, provides information on the objectives, proposed targets and research methodology of the doctoral thesis. Also, the materials, methods and equipment needed both for the development of the materials and their characterization are presented.

Chapter IV, entitled **EXPERIMENTAL RESEARCH ON THE OBTAINING AND CHARACTERIZATION OF MATERIALS BASED ON ZrO2 DOPED WITH RARE EARTHS,** primarily aimed at the study of the synthesis of powders based on ZrO_2 doped with 8% Y_2O_3 and co-doped with different controlled amounts (4,6,8 wt%) of a single REE (REE= La, Nd, Sm și Gd). Thus, 12 types of powders were developed by the hydrothermal method: MxZY4La, MxZY6La, MxZY8La, MxZY4Nd, MxZY6Nd, MxZY8Nd, MxZY4Sm MxZY6Sm, MxZY8Sm și MxZY4Gd, MxZY6Gd, MxZY8Gd.

Before the actual synthesis, the thermodynamic prediction of hydrothermal reactions was used, which was useful in understanding the formation and stability of all species under given process conditions (reaction temperature, pressure, reactant concentration and pH). It was thus possible to identify the feasible regions for the hydrothermal synthesis of materials.

The obtained powders were characterized from the point of view of: chemical composition, phase purity and crystal structure, thermal stability and microstructure, to confirm the feasibility of the process.

The behavior of the 12 types of powders during heat treatment was studied ($Tt_{ratament}$ = 400 °C/ 800 °C/ 1000 °C/ 1200 °C/ 1400 °C) by highlighting the evolution of the phases and the morphology of the powders. For this purpose, 60 heat-treated powders were obtained. A batch of powders has been selected (MxZY6RE - $T_{tratament}$ = 1000°C) for tracking thermal conductivity properties.

The experiments continued by developing two types of powders:

- ZrO_2-based powder doped with 8% by weight mixture of synthetic REOs with a ratio corresponding to natural occurrence in selected Ce-rich monazite concentrates. It resulted in a type of powder referred to hereafter as ZrO2CeRO.powder doped with 8% by weight mixture of synthetic REOs with a ratio corresponding to the natural occurrence in selected La-rich monazite concentrates. It resulted in a type of powder hereafter referred to as ZrO2RE.

- ZrO_2-based powder doped with 8% by weight mixture of synthetic REOs with a ratio corresponding to natural occurrence in selected Ce-rich monazite concentrates. It resulted in a type of powder referred to hereafter as ZrO2CeRO.

The obtained powders were characterized from the point of view of: chemical composition, phase purity and crystal structure, thermal stability, microstructure and thermal conductivity.

Chapter V, entitled, **EXPERIMENTAL RESEARCH ON THE OBTAINING AND CHARACTERIZATION OF THERMAL BARRIERS,** presents the obtaining by the EB-PVD process of two types of thermal barriers based on ZrO_2 doped with a mixture of rare earth elements.

Therefore, multilayer coatings were obtained on NIMONIC 80 super-refractory alloy support, which have the following architecture:

- Nimonic/NiCrAlY/Al_2O_3/ZrO2RE/LZO/GZO;
- Nimonic/NiCrAlY/Al_2O_3/ZrO2CeRO/LZO/GZO).

The TBC samples obtained were characterized from the point of view of: microstructure, morphology, tribological properties, roughness and thermal shock behavior.

Chapter VI, entitled **CONDUCTING A THERMAL BARRIER MARKET STUDY** presents a market study using data provided by specialist firm Maya Research Analysis U.K., with data collected for the period 2016-2020 and forecasts for the period 2021-2027.

Therefore, this chapter has graphed and interpreted TBC data globally by type, application and region, helping to create an overview of the field.

So, the **novelty and originality** of the doctoral thesis is given by the integration of emerging technologies, hydrothermal synthesis with that of physical vapor deposition by electron beam (EB-PVD) with the aim of demonstrating the efficiency of using synthetic mixtures of rare earths (mixture that simulates the mixture found in monazite) as dopants in ZrO_2-based materials with applications in thermal barrier coatings.

This integration also denotes the **interdisciplinary nature of the thesis.**

For the first time, both the potential of hydrothermal synthesis in obtaining complex multi-component powders based on a mixture of rare earths (which simulates the composition of monazite), such as ZrO2RE, ZrO2CeRO, as well as the potential of the EB-PVD process in obtaining multilayer coatings, will be exploited. of the type of thermal barriers. The thesis ends with bibliographic references, the list of works published in the field of the thesis, as well as the list of supported communications.

.

CHAPTER I. CURRENT STATUS ON CRITICAL MATERIALS AND THEIR ROLE IN GREEN ENERGY. RARE EARTHS AS CRITICAL MATERIALS

1.1 The context of criticality of raw materials

Since the first decades of the 20th century, based on the fear of supply interruption, a discourse related to strategic raw materials has been noted. Thus, due to the mass industrial warfare of the First World War (1914–1918), strategic thinking began regarding mineral raw materials considered essential for the projection of military power and for national trade [7].

Before World War II (1939-1945) broke out, the term "criticality" was first used in the US in July 1939 in the context of raw material stockpile legislation [3-4]. Strategic and critical materials" were "materials that would be needed to supply the essential military, industrial, and civilian needs of the United States during a national emergency and are not found or produced in the United States in sufficient quantities to meet that need " [10]. During that period, the US Administration decided to hold a stockpile of 42 raw materials for a military emergency. The geopolitical situation relaxed after the end of the Cold War.

Today, the term "criticality" no longer refers only to military technologies and national economies, it can refer to a regional or global level, being able to take into account, in addition to the strategic importance, political, ecological, ethical, social, and technical aspects of criticality [11].

1.2 Criticality assessment at the general level

1.2.1 Evaluation indicators

In order to be able to evaluate the criticality, it is necessary to establish certain indicators. In general, from the literature review and the opinions of expert groups, these indicators are divided into supply indicators and economic indicators [4].

The first criterion consists of a "supply indicator" and an "economic indicator".. "Supply risk" and "vulnerability" are included in the "supply indicator" and "economic risk" is set as a sub-indicator of the "economic indicator". The three sub-indicators are defined as the second criterion, and the indicators are subdivided into a total of eleven indicators..

1.2.2 Criticality assessment methods

The way in which critical raw materials are identified in many studies is represented in figure 1.2.

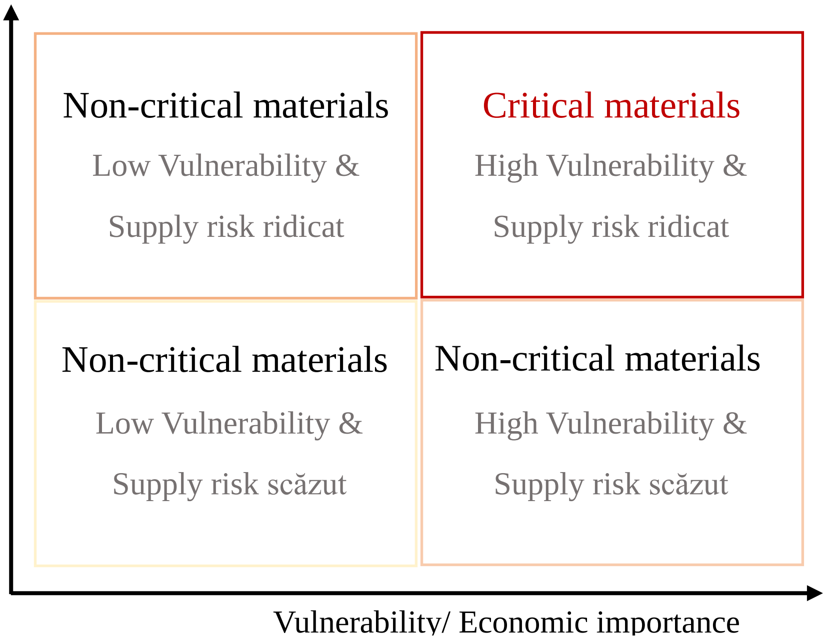

Figure 1. 1. Criticality assessment scheme showing how critical raw materials are identified.

1.3 The Context of Criticism at the European level

The European Ecological (Green) Pact, adopted on 11 December 2019, represents a new growth strategy for Europe, which aims to transform the EU into a society with a modern, competitive and resource-efficient economy. Thus, access to resources is a security strategy to meet the ambitious goal of being the world's first climate-neutral continent by 2050 [20]. Industry has an important role in this challenge. The new industrial strategy for the EU adopted in 2020 brings to the fore the fact that with the transition of European industry towards climate neutrality, the current dependence on fossil fuels could be replaced by a dependence on raw materials. Thus, it is proposed to strengthen the open strategic autonomy of Europe [21].

The activity of the European Commission to address the growing concern of securing valuable raw materials for the EU economy continues.

In addition to all these challenges, the crisis caused by the COVID-19 pandemic has also been added, which has clearly shown Europe's dependence on non-EU suppliers for critical raw materials, revealing how quickly and how deeply global supply chains can be disrupted, having a negative impact on the industry and other sectors.

One of the initiative's priority actions was the creation of an EU-wide list of critical non-energy raw materials [22].

The first list was established in 2011 and is updated every three years. The latest 2023 list presents the assessment of 70 raw materials, comprising 67 individual materials and three groups of materials: ten heavy rare earth elements (HREE), five light rare earth element (LREE) and five metals from the platinum group (PGM), 87 individual raw materials in total. Four new materials were evaluated: neon, krypton, xenon and wood [23].

The criticality of a raw material is determined by comparing the main parameters, Economic Importance (EI) and Supply Risk (SR) with the criticality threshold values established, based on the scaled results of the criticality assessments. Raw materials that meet or exceed the thresholds set for both parameters are classified as critical raw materials (CRM). From the point of view of criticality, there is no ranking order of raw materials [23].

Compared to the list published in 2020, the one in 2023 presents 6 more critical raw materials (arsenic, feldspar, helium, manganese, but also copper and nickel considered to be strategic elements). Indium and natural rubber are no longer among the elements to be considered critical.

China is the leading global supplier of critical raw materials, which includes all REEs and other critical raw materials such as magnesium, tungsten, antimony, gallium, and germanium, among others. China is also a major consumer of several of these critical raw materials, eg: HREE, LREE, antimony, PGM, natural graphite, magnesium, tungsten, etc. [26-27].

All these raw materials, assessed as critical by the European Commission, are essential prerequisites for the development of strategic sectors, such as: electric mobility, renewable energy, digital technologies, defense and aerospace.

EU industry is currently highly dependent on imports for many of its raw materials, making it in some cases highly exposed to vulnerabilities along the supply chain.

In table 1.11. the use of the most important materials in strategic technologies are presented.

Table 1. 1. Use of materials in strategic technologies [28].

Supply risk	Material									
5,98	LREEs		✓	✓	✓		✓	✓		✓
5,63	HREEs		✓	✓	✓		✓	✓		
3,91	Mg		✓				✓	✓	✓	✓
3,90	Nb	✓		✓				✓	✓	
3,89	Ge					✓		✓		✓
3,55	P	✓					✓	✓		✓
3,19	B		✓	✓	✓	✓	✓	✓	✓	✓
3,09	Sc							✓	✓	
2,57	St		✓				✓	✓		
2,54	Co	✓	✓	✓			✓	✓	✓	✓
2,38	PGMs		✓				✓	✓		✓
2,29	Be							✓		
2,27	C(grafit)	✓	✓				✓	✓		✓
2,22	Bi						✓	✓		✓
2,01	Sb						✓	✓		
1,79	In					✓	✓	✓		
1,69	V		✓				✓	✓	✓	✓
1,64	Li	✓	✓				✓	✓		
1,61	W						✓	✓	✓	
1,36	Ta						✓	✓		
1,15	F	✓					✓	✓		
1,26	Ti	✓	✓				✓	✓	✓	✓
1,26	Ga					✓	✓	✓		✓
1,19	As		✓				✓	✓		✓
1,18	Si	✓	✓		✓	✓	✓	✓	✓	✓
1,12	Hf							✓	✓	
0,94	Mo		✓	✓		✓	✓	✓	✓	✓
0,93	Mg	✓	✓	✓			✓	✓	✓	✓
0,90	Sn	✓				✓	✓	✓		✓
0,86	Cr		✓				✓	✓	✓	✓
0,83	Zr		✓				✓	✓	✓	✓
0,68	Ag		✓			✓	✓	✓		✓
0,59	Al	✓	✓	✓	✓	✓	✓	✓	✓	✓
0,51	Te					✓	✓	✓		✓
0,49	Ni	✓	✓			✓	✓	✓		✓
0,46	Fe	✓	✓	✓	✓	✓	✓	✓	✓	✓
0,41	Se	✓	✓				✓	✓		✓
0,34	Zn					✓	✓	✓		
0,34	Cd					✓	✓	✓		✓
0,32	Cu	✓	✓	✓	✓	✓	✓	✓	✓	✓
0,19	Au		✓				✓	✓		✓
0,09	Pb	✓		✓		✓	✓	✓		✓

Among these critical materials, rare earths are increasingly important in modern industry. In the transition to a green economy, rare earth elements (REE) are becoming increasingly important

1.5 The rare earths

Rare earths typically refer to rare earth elements (REEs), which are a group of 17 elements in the periodic table comprising 15 elements with atomic numbers 57 to 71 (called lanthanides), plus scandium (Sc, 21) and yttrium (Y, 39) [63-65]. These elements are considered REEs because they occur in the same deposits as the lanthanides, also exhibiting similar chemical properties [66].

Generally, REEs are divided into two broad categories, namely light rare earth elements (LREE) (from La to Gd) and heavy rare earth elements (HREE) (from Tb to Lu) [73].

The most important sources of combined REE in mineral deposits are monazite and bastnaesite. Monazite is a phosphate mineral, while bastnaesite is a fluorinated carbonate mineral that contains various REE [79].

China controls much of the rare earth supply chain. It handles 91% of the refining and 87% of the oxide separation [82].

Rare earth elements are also called "Vitamins of modern industry" because they are extremely important in the development of high-tech gadgets, but also for the development of several applications such as ceramics, batteries, catalysts, etc. [66].

CHAPTER II. THE CURRENT STATE OF RESEARCH IN THE FIELD OF THERMAL BARRIERS BASED ON ZRO_2 DOPED WITH RARE EARTHS

2.1 Obtaining ceramic material based on ZrO_2 doped with rare earths

2.1.1 Zirconium Dioxide

Zirconium dioxide (ZrO_2), also known as zirconium oxide or zirconia, is a ceramic material of great technological importance due to its advanced multidimensional properties, such as: low thermal conductivity, high temperature stability, corrosion resistance, chemical inertness, high ionic conductivity and biocompatibility [87-89]. Due to these properties, ZrO_2 plays an important role in applications such as: thermal barrier coatings [90], solid oxide fuel cells [91], gas sensors [92], catalysis [93], medical prostheses [94], and devices memory [95].

Depending on the temperature conditions, pure zirconia is found in three polymorphic forms, namely:

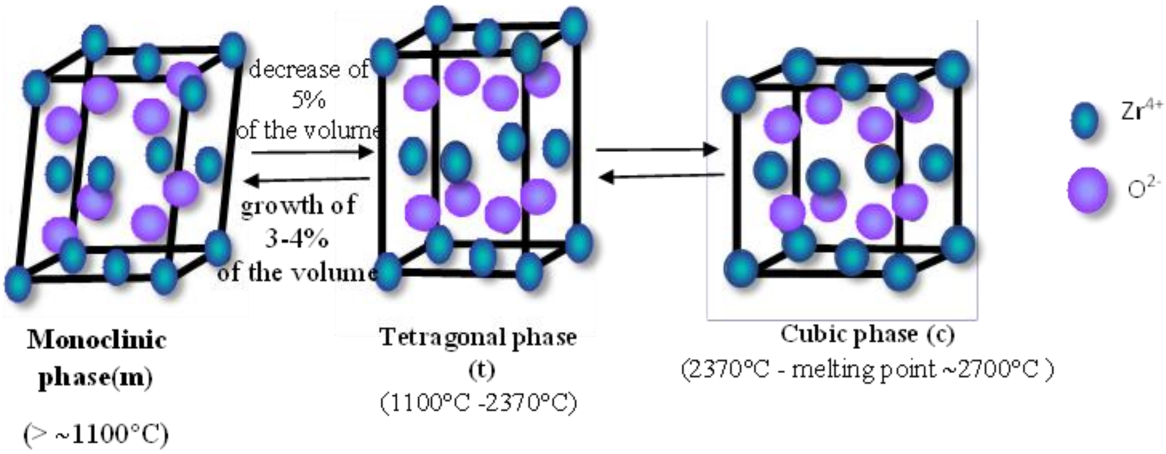

Figure 2. 1. The three common crystal structures of zirconia

2.1.2 Stabilization of zirconia by doping

Following the high stresses during the cooling period, pure ZrO_2 suffers micro-cracks that strongly affect the mechanical properties. This type of problem can be overcome by adding oxides (higher cations with lower valence than Zr^{4+}) such as MgO, CaO and Ln_2O_3 (Ln: all transition metals in the lanthanum series of the periodic table of elements) as stabilizers, to zirconium oxide to stabilize tetragonal and/or cubic phases at room temperature [98-100].

The use of rare earth oxides (REOs) as dopants can avoid grain coarsening due to interface segregation in doped zirconia ceramics, thereby improving its thermo-mechanical properties.

2.1.4. Synthesis and properties of ZrO_2 ceramic powders doped with REO

Regarding the doping of zirconia with mixed rare earth oxides, different synthesis methods have been proposed. A summary of the influence of the synthesis route on the structure and morphology of ZrO_2 doped with rare earth oxides is presented in Table 2.2.

Table 2. 2. Morphological and structural properties of different materials based on ZrO_2 doped with rare earth oxides

Nr.	Material	Synthesis type	Morphological and structural properties	Ref
1	ZrO_2 doped with 8 wt% rare earths (Ce, Gd and Y).	Sol-gel	Monoclinic and tetragonal phases; by doping with RE ions, the crystallite size is reduced (D = 6752 nm for undoped ZrO_2, D = 4640 nm for doped ZrO_2).	[111]
2	ZrO_2 dopaed with Ce, ZrO_2 dopaed with Dy	Co-precipitation	Tetragonal and monoclinic phases; doping with RE ions, the crystallite size is reduced (D = 12 nm for undoped ZrO 2, D = 9 nm for ZrO 2 /Dy, D = 6 nm ZrO 2 /Ce)	[112]
4	YSZ doped with 1 mol% RE_2O_3 (RE =La, Nd, Gd, Yb) and co-doped with 1 mol% Yb_2O_3 (1RE1Yb-YSZ)	Co-precipitation	The tetragonal phase	[113]
10	xmol%Sc_2O_3 - 1,5 mol%Y_2O_3 -ZrO_2 (x = 4.5, 5.5, 6.5,	Co-precipitation	increasing the content of Sc_2O_3, phase stability also increases.	[114]
3	(Gd (1–9 mol%) doped with ZrO2	Burning the solution	D = 25–35 nm	[89]
5	partial substitution of Y_2O_3 with the equivalent Ln_2O_3 (Ln = Nd, Sm, Gd in ceramics ZrO_2 -Nb_2O_5 -Y_2O_3	Eeacția în stare solidă	faza tetragonală	[115]
	x mol% ZrO_2 -Gd_3NbO_7 (x = 0, 3, 6, 9, 12)	Solid state reaction	D = 2–20 μm	[116]
6	ZrO_2–Ta_2O_5 Y_2O_3–Ln_2O_3 (Ln =Nd, Sm or Gd) ZrO_2 – doped with (8,3% mol Ta_2O_5 + 8,3% mol Y_2O_3. 1 mol.% Ln_2O_3 substituted 1 mol% Y_2O_3	Solid state reaction	All compositions consisted only of the tetragonal phase (t) when 1 mol % Ln2O3 was replaced by 1 mol % Y2O3. Also, the introduction of Ln2O3 resulted in a decrease in grain growth.	[117]
7	ZrO_2-Ln_2O_3 (Ln = Sm, Yb)	Colloidal chemical synthesis and spark plasma	no phase transformation occurs during heating	[103]

		sintering		
8	$ZrO_2 9.5Y_2O_3 5.6Yb_2O_3 5.2Gd_2O_3$	Chemical precipitation	excellent stability of the tetragonal phase (of thermal cycling at 1300 °C for 50 hours)	[98]

2.2 Obtaining thermal barriers based on ZrO_2 doped with rare earthsa

2.2.1 General thermal barriers

Thermal barrier coatings are complex coating systems, used as a heat barrier to stop its progression throughout the material, reducing the substrate temperature between 100 ºC and 300 ºC [118]. TBC plays the significant role of protecting internal combustion engine parts [119-125] metal parts of gas turbine engines (such as vanes, valves, and combustion chambers), [126-130], and others operating at higher temperatures, providing significant resistance to corrosion, erosion and oxidation at high temperaturese [131-132].

The thermal barrier coating system used to protect Ni-based superalloys is shown in Figure 2.3. TBC generally consists of two key layers: an oxidation-resistant bond layer (BC) such as MCrAlY (M=Ni, Co)) and a ceramic top layer (TC). The adhesion layer is deposited between the metal substrate and the top layer to protect the substrate from oxidation and corrosion at high temperatures but also to help the coupling of the ceramic coating layer and the metal substrate, balancing the thermal mismatch between the top layer and the substrate. Due to the high temperatures, a thermally grown oxide (TGO), predominantly alumina) is formed as a reaction product between the upper layer and the bonding layer [135-136].

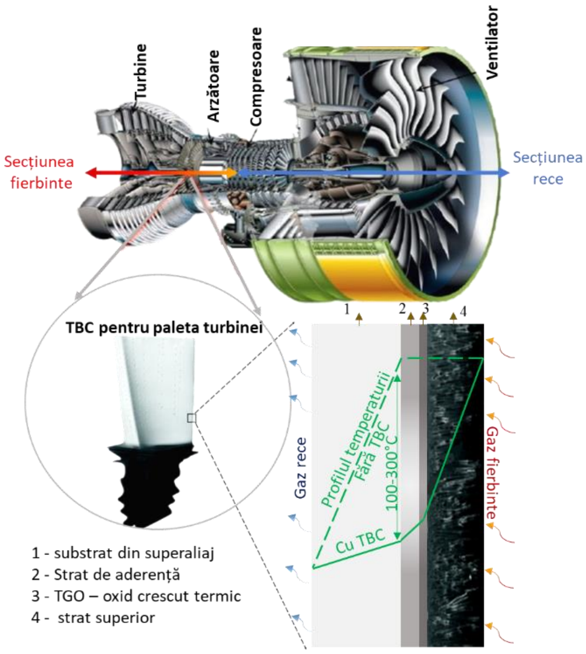

Figure 2. 1. Schematic of a typical thermal barrier coating for gas turbine blades.

2.2.2 Deposition techniques

EB-PVD and APS are the best techniques for obtaining TBCs and various multilayer coatings from a large class of different materials.

A specific aspect of EB-PVD coatings is related to their columnar microstructure (figure 2.5 a) which determines the behavior of the coating during its lifetime. This structure leads to a very high tolerance to deformation, which occurs during thermal cycling changes, but also reduces the thermal expansion mismatch between BC and TC, promoting a longer lifetime of the TBC system [137,148,149].

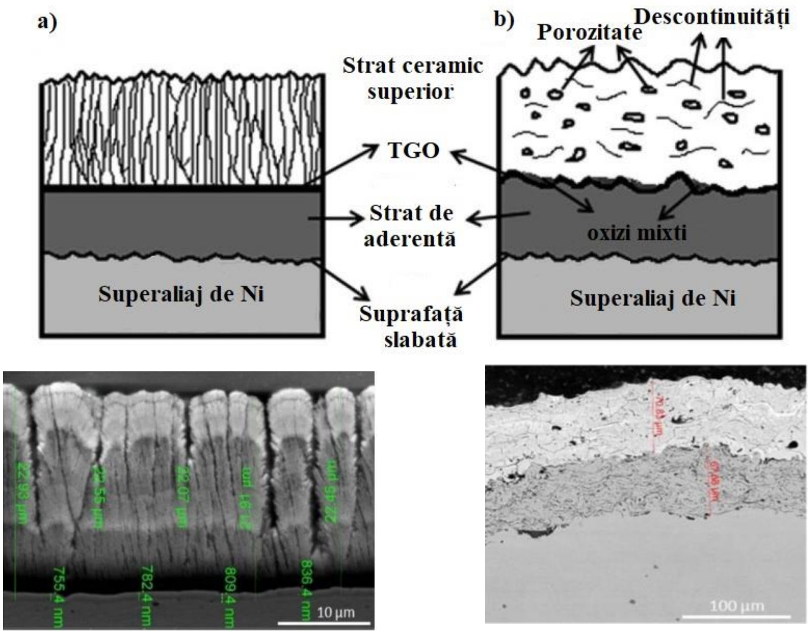

Figure 2. 2. Schematic of TBC structures obtained by: (a) EB-PVD and (b) APS and SEM micrographs showing the typical morphology of YSZ coatings deposited on Nimonic 80A substrate: (a) columnar structure of EB-PVD coating and (b) flat morphology of APS coverage [151].

2.2.3. Thermal barrier coatings based on ZrO2 doped with REO

In recent years, there is an increasing theoretical and practical interest in the use of various REO mixtures as dopants for high-temperature ceramics, especially for ZrO_2-based thermal barrier coatings (TBCs) used in aeronautics and co- power generation. The use of mixed REOs can increase the working temperature of TBC, due to the formation of tetragonal and cubic solid solutions with higher melting temperatures, avoiding grain size thickening due to interface segregation, increasing its ionic conductivity and sinterability.

2.2.4. Multi-layer ceramic coatings

To improve the lifetime of the coatings, two-layer ceramic coating systems have been developed. The bottom layer is YSZ and the top layer should be a material with high temperature phase stability. Such types of materials are pyrochlore and perovskite [151]. A schematic of such a proposed structure is shown in figure 2.6.

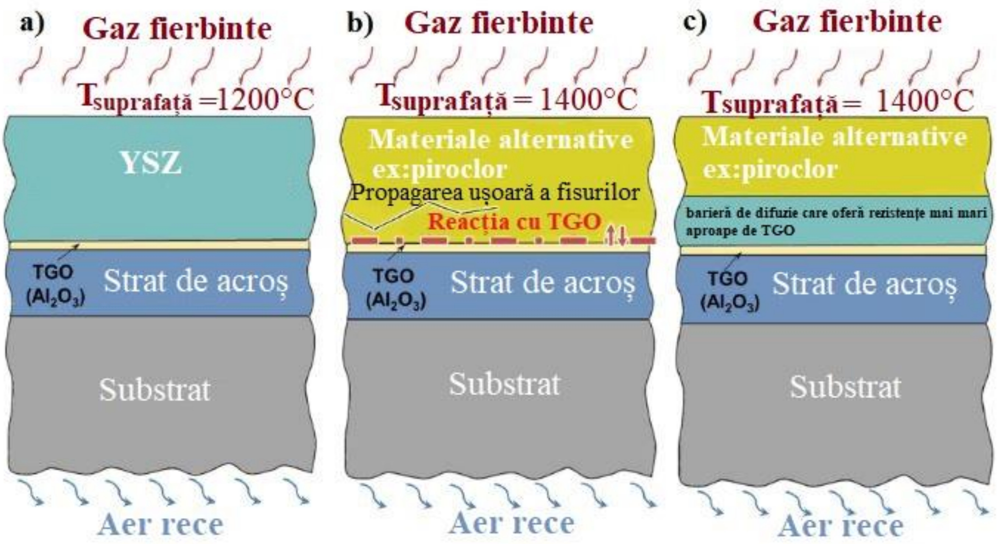

Figure 2. 3. Comparison of conventional single-layer TBC (a) and single-layer alternative material (b) with double-layer TBC (c), which improve the ability to work at higher operating temperatures [151].

2.3 Thermal barriers based on advanced lanthanum zirconate (LZO) and gadolinium (GZO) oxide systems (GZO)

Rare earth zirconates (RZOs) with pyrochlore structure are currently considered emerging TBC materials due to the lack of phase transitions up to the melting point (around 2300 °C) and lower intrinsic thermal conductivity (1,4 up to 1,6 $W \cdot m^{-1} \cdot K^{-1}$ compared to ~2,3 $W \cdot m^{-1} \cdot K^{-1}$ for YSZ ceramics. The low thermal conductivity of the pyrochlore ($A_2B_2O_7$) structure is determined by the high concentration of oxygen vacancies and the ionic mass difference between $Ln3^+$ and Zr^{4+} that results in phonon scattering [167-176]. Disadvantages are lower tensile strength (0.9–1.3 $MPa \cdot m^{0.5}$) than that of YSZ (~3 $MPa \cdot m^{0.5}$) [158-168]and larger differences in thermal expansion coefficients that occur during the thermal cycle, reducing TBC adhesion [167].

CHAPTER III. RESEARCH OBJECTIVES AND METHODOLOGY

3.1 The objectives of the doctoral thesis

Currently, there is increased interest from researchers in the sustainability issues related to REE mining and treatment. Researchers working in this field are often concerned with the impact of REEs on environmental systems and study the life cycle assessment of REEs because they can be a source of contamination in several ecological systems [186] also generating several health risks human [187].

Starting from this aspect, the basis of the development of the doctoral thesis was the question "What would happen if these REO were used as they are found in ores?!"

Therefore, the objective of the thesis is to demonstrate the potential of using mixtures of rare earth oxides (REOs) (mixture that simulates the natural composition of monazite concentrates), as dopants in the design of zirconia-based coatings, which contribute to a efficient use of critical raw materials, with an impact on ensuring the transition to climate neutrality.

This new concept can also have a high impact in reducing the consumption of reagents by eliminating the individual extraction of rare earth oxides, resulting in a reduction in the cost of materials used in high tech applications.

In order to ensure the fulfillment of the main objective of the doctoral thesis, the following 6 specific objectives were considered:

O1: Elaboration of a literature study on critical materials and their role in green energy. Rare earths as critical raw materials;

O 2: Elaboration of a literature study on obtaining thermal barriers based on ZrO2 doped with rare earths;

O 3: Evaluation of the influence of La_2O_3, Nd_2O_3, Sm_2O_3, Gd_2O_3 oxides used as dopants on the structure and morphology of ZrO_2 ceramics doped with Y_2O_3;

O 4: Demonstration of the potential of using the synthetic mixed mixture of REO to obtain two types of ZrO2-based materials in the form of powders (ZrO_2RE,ZrO_2CeRO);

O 5: Demonstration of the potential of using the synthetic mixed mixture of REO to obtain two types of thermal barriers (Nimonic/NiCrAlY/Al_2O_3/ZrO_2RE/LZO/GZO, Nimonic/NiCrAlY/Al_2O_3/ZrO_2CeRO/LZO/GZO);

O 6: Development of a market study on thermal barriers.

3.2 Research methodology

The research methodology, the work plan, the experiments and the actual characterizations were designed and carried out within the framework of the National Research-Development Institute for Non-Ferrous and Rare Metals.

The doctoral thesis work plan comprises two parts that aim to achieve specific objectives. **The first part** is one related to the **current state of knowledge**, which includes chapters one and two, in which the current state of the research topic is presented, through a descriptive analysis of the research in the field, based on a laborious documentation.

The second part of the thesis is given by the **author's personal contribution** and includes the experimental research of the doctoral thesis, as well as a market study.

Within the doctoral thesis, the achievement of the following goals was aimed at:

- **12 types of powders based on ZrO2** doped with 8% Y2O3 and co-doped with 4/6/8% RE (RE=La, Nd, Sm, Gd): *MxZY4La, MxZY6La, MxZY8La, MxZY4Nd, MxZY6Nd, MxZY8Nd, MxZY4Sm MxZY6Sm, MxZY8Sm and MxZY4Gd, MxZY6Gd, MxZY8Gd;*
- **60 heat-treated powders:** *MxZY4La, MxZY6La, MxZY8La, MxZY4Nd, MxZY6Nd, MxZY8Nd, MxZY4Sm MxZY6Sm, MxZY8Sm and MxZY4Gd, MxZY6Gd, MxZY8Gd at T=400/800/1000/1200/1400 °C;*
- **2 types of powders based b:** *ZrO2RE(*element majoritar La), *ZrO2CeRO* (element majoritar Ce)
- **6 types of pressed pills:** *P1-MxZY6La, P2-MxZY6Nd, P3-MxZY6Sm, P4-MxZY6Nd, P5- ZrO2RE; P6- ZrO2CeRO*;
- **2 types of thermal barrier samples:** *Nimonic/NiCrAlY/Al2O3/ZrO2RE/LZO/GZO; Nimonic/NiCrAlY/Al2O3/ZrO2CeRO/LZO/GZO*

In the ZrO2RE, ZrO2CeRO samples, 8 wt% Y_2O_3 commonly used as TBC dopant was replaced by 8% synthetic REOs mixture with a ratio corresponding to the natural occurrence in selected La^- and Ce^- rich monazite concentrates, respectively.

The stages that were the basis of the doctoral thesis development are presented below in figure 3.1

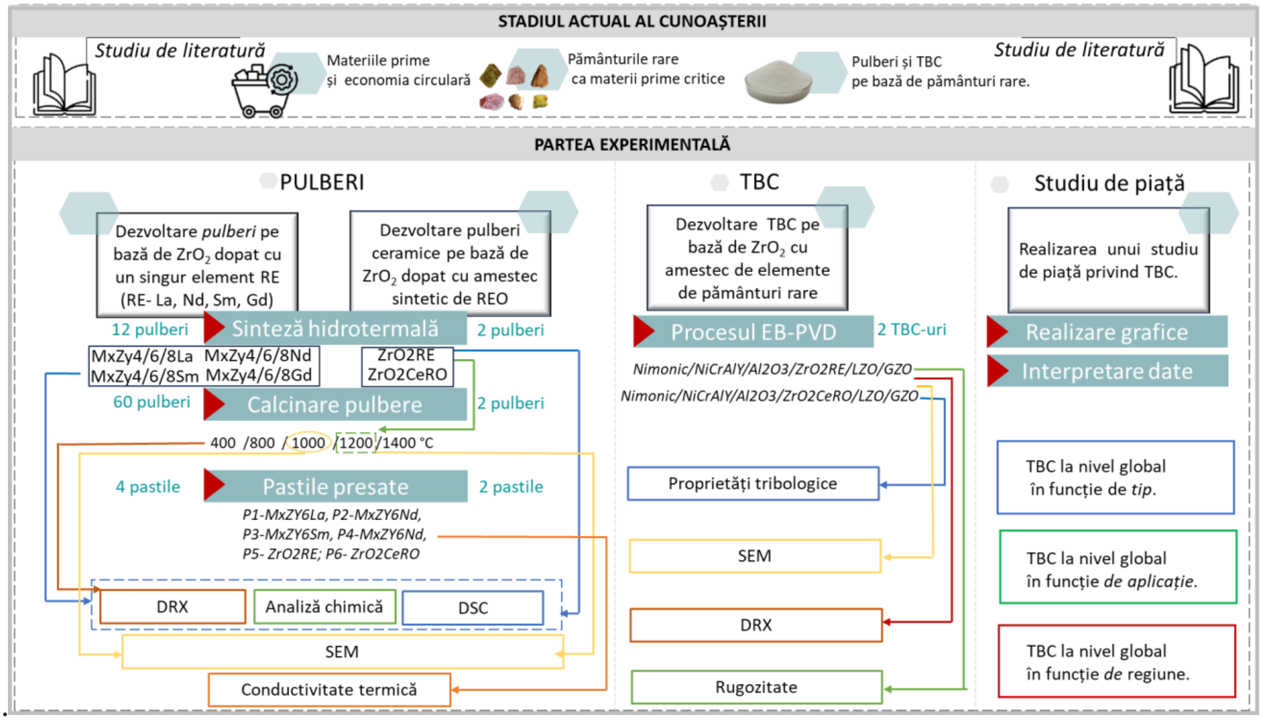

Figura 3. 1 Schematic representation of the work plan.

In order to achieve the proposed general objective, in this thesis the most relevant investigation methods and techniques were used to provide the results in order to demonstrate the potential of use of the synthetic mixed mixture of REO: chemical analysis of the powders, microstructure and morphology, thermal stability , thermal conductivity, as well as determining the tribological properties of TBCs, thermal shock behavior.

CHAPTER IV. EXPERIMENTAL RESEARCH ON THE OBTAINING AND CHARACTERIZATION OF MATERIALS BASED ON ZRO2 DOPED WITH RARE EARTHS

4.1 Obtaining powders based on ZrO_2 doped with REO

4.1.2. Hydrothermal synthesis

All nanostructured powders were synthesized in one step by the hydrothermal method at moderate temperatures (max. 250 ◦C) and pressures (max. 40 atm).

4.1.3. Thermal treatment of powders

The next step was to evaluate the phase stability of MxZY 4/6/8La, MxZY4/6/8Nd, MxZY, 4/6/8Sm, MxZY 4/6/8Gd powders. Therefore, they were heat treated at different temperatures (400 °C/ 800 °C/ 1000 °C/1200 °C/1400 °C) for 60 minutes and their phase compositions were analyzed.

As a result, the ZrO2RE and ZrO2CeRO powders were subjected to heat treatment at the temperature considered optimal, that of 1200 °C for 60 minutes, also analyzing the phase composition.

4.1.1. Obtaining and sintering pellets

A manual press is used to obtain pellets of approximately 20 mm size. Thus, 6 types of pressed pills were obtained, named below: P1-MxZY6La, P2 - MxZY6Nd, P3 - MxZY6Sm, P4 - MxZY6Gd, P5 - ZrO2RE, P6 - ZrO2CeRO.

4.2 Characterization of ceramic powders based on ZrO2 doped with REO

In this chapter, the results regarding the development of individual and multicomponent REO-doped zirconia simulating the existing composition in some selected monazite concentrates after removal of radioactive elements (Th, U and Ra) were presented.

4.2.1. Characterization of powders with unitary REO dopant

ZrO_2 powders doped with 8% Y_2O_3 and co-doped with 8% synthetic REO mixture (containing La, Gd, Y, Nd, Gd and Yb with a ratio corresponding to the natural occurrence in selected concentrates of La-rich monazite and Ce, respectively) were prepared by a hydrothermal method at moderate temperatures (max. 250 °C) and pressures (max. 40 atm.). The XRD pattern of this powder corresponds to a monophasic tetragonal ZrO_2 solid solution, consisting of granular aggregates with sizes up to tens of microns.

Tabel 4. 1. XRD spectra for MxZY 4/6/8La, MxZY4/6/8Nd, MxZY, 4/6/8Sm, MxZY 4/6/8Gd samples thermally treated at different temperatures.

MxZy4/6/8La

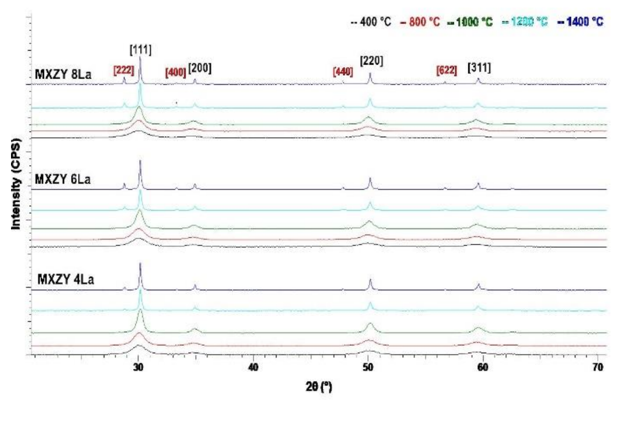

MxZy4/6/8Nd

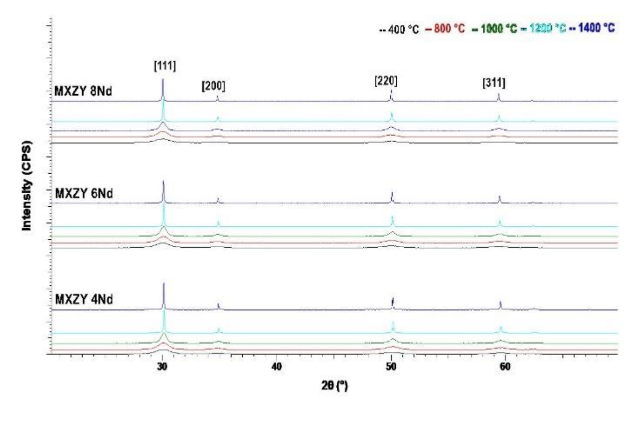

MxZy4/6/8Sm

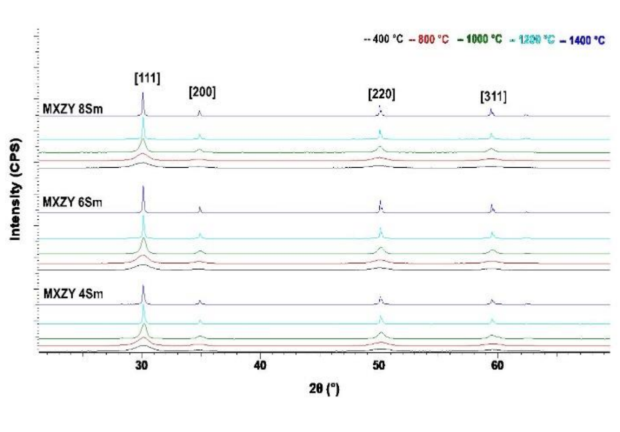

MxZy4/6/8Gd

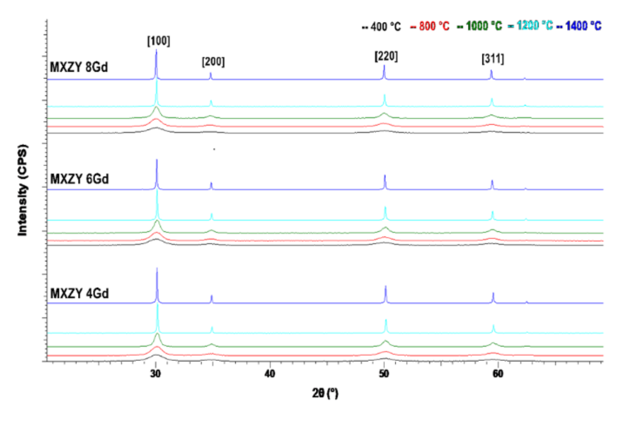

SEM analysis shows that nanopowders with irregular shapes are formed in all systems and no significant grain growth is observed after calcination. Figure 4.5 shows as an example only the morphology of YSZ powders of 8% by weight co-doped with 4/6/8% La_2O_3, obtained by hydrothermal processes and after calcination at 1000 ° C, including the grain sizes of all samples.

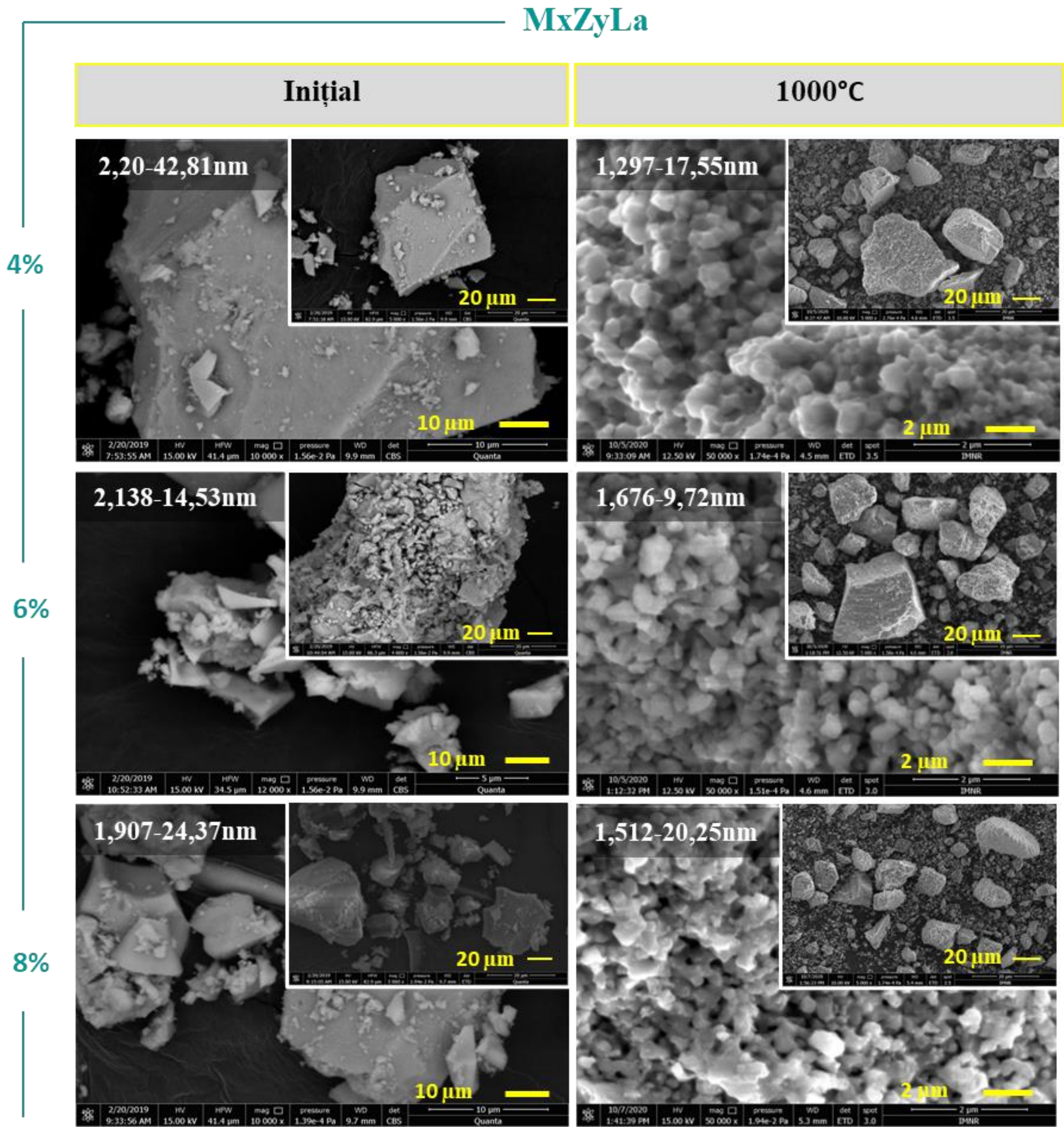

Figure 4. 1. Representative SEM images of MxZy4La, MxZy6La, MxZy8La material at different magnifications.

Thermal analysis was used to follow the thermal stability of the hydrothermally synthesized powders and the phase transformations during heat treatment. Only the TG and DSC graphs of the MxZy4/6.8%La powders heated from ambient temperature to 1450 °C are shown in Table 4.6, with the specification that for the other samples the graphs are similar.

Table 4. 2. DSC-TG analysis of MxZy4/6/8%Ln.

MxZy4La	*MxZy6La*	*MxZy8La*
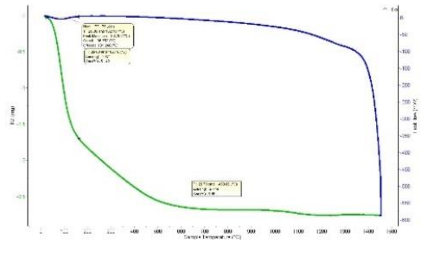	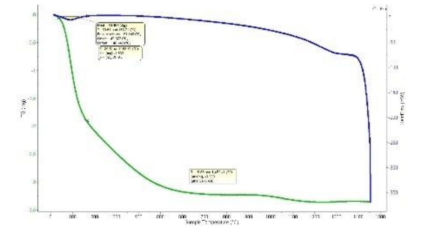	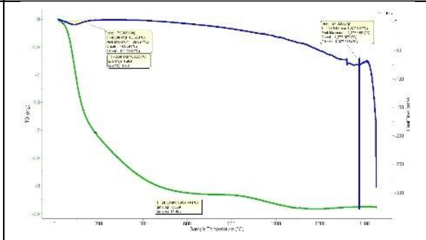

DSC-TG measurements show a continuous mass loss up to about 600 °C and an endothermic peak around 80–90 °C, revealing a dehydration process of the materials, which is in agreement with other literature studies [73].

Thermal conductivity

The obtained values range from 0.305 W/mK, for pellets co-doped with La, to 0.38 W/mK for pellets co-doped with Gd.

The thermal conductivity values obtained are similar to those obtained in the work [193] in which the materials RE_2O_3 (RE = La, Yb, Ce and Gd) and ZrO_2 co-doped with Y_2O_3 were obtained by sol-gel methods. The thermal conductivities for RE-YSZ powders (RE = La, Yb, Ce and Gd) were: 0.5181, 0.4215, 0.4851, 0.5187 and 0.5347 W/mK, respectively..

4.2.2. Characterization of ZrO_2 powders doped with REO mixture

Chemical analysis

The chemical analysis of the powders synthesized under hydrothermal conditions is presented in Table 4.6. and is in accordance with the designed compositions. The concentration of Zr, Y and Ln in the mother liquor resulting from the filtration of the hydrothermal reaction products and in the washing waters was in all cases $<10^{-3}$ g ·L^{-1} .

XRD

The XRD spectra for the ZrO2CeRO and ZrO2RE powders are shown in figure 4.14 and 4.15, respectively.

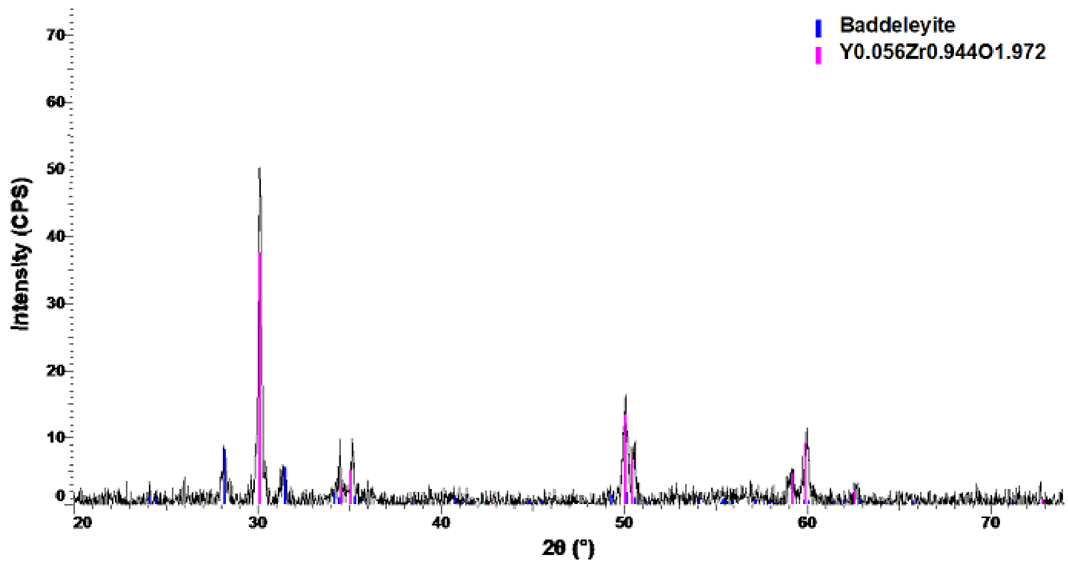

Figure 4. 2 XRD spectrum for ZrO2 CeRO powder heat treated at 1200°C.

Compound name	Formula	Identified card	Crystallization system
Baddeleyite	ZrO_2	PDF 04-004-4339	Monoclinic
Zirconium Oxide	Ss baza ZrO_2	PDF 01-079-1769	Tetragonal

The hydrothermally synthesized ZrO2CeRO powder has the ZrO2 solid solution with tetragonal structure as the main phase and monoclinic zirconium oxide (Baddeleyite) as the secondary phase..

Figura 4. 3. XRD spectrum for ZrO2RE powder heat treated at 1200 °C.

Compound name	Identified card	Formula	Crystallization system
Zirconium Yttrium Oxide	PDF 00-060-0505	ss((Y,La,Gd,Nd,Sm,Yb)$_2$ O$_3$) (ZrO_2)	tetragonal

The hydrothermally synthesized ZrO2RE powder has the solid solution ss((Y,La,Gd,Nd,Sm,Yb)2 O3) (ZrO2) with tetragonal structure as the unitary phase.

Analiza SEM

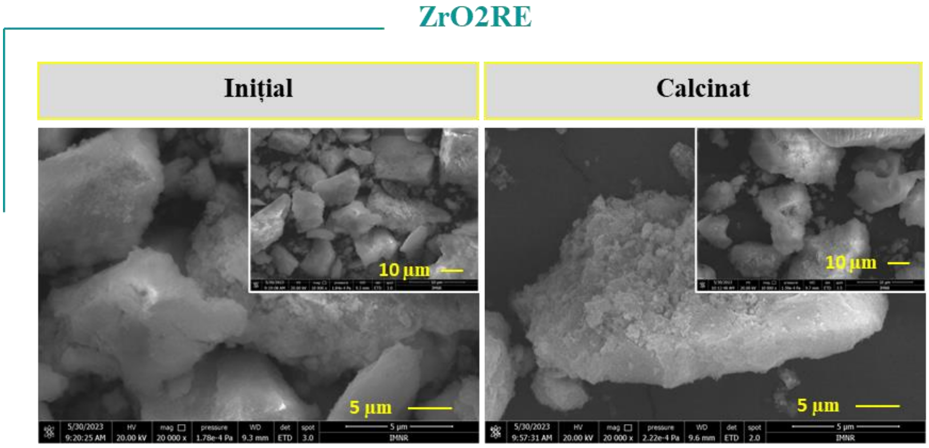

Figure 4. 4. Representative SEM images of ZrO2RE material.

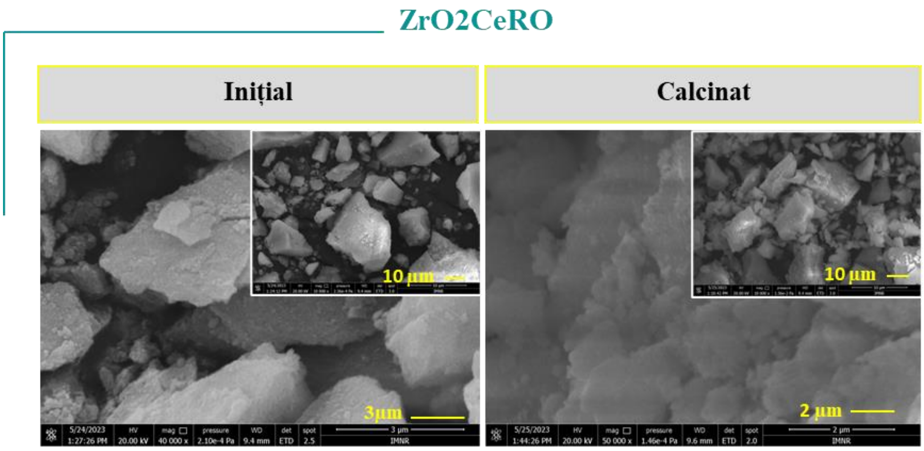

Figure 4. 5. Representative SEM images of ZrO2CeRO material.

The scanning electron microscopy images shown in Figures 4.16 and 4.17 show that nanopowders with irregular shapes are formed in all systems and no significant grain growth is observed after calcination.

Energy dispersive X-ray spectroscopy (EDS) was used to determine the chemical composition of the powders used in this study. The EDS results are shown in Figures 4.19 and 4.19.

DSC analysis

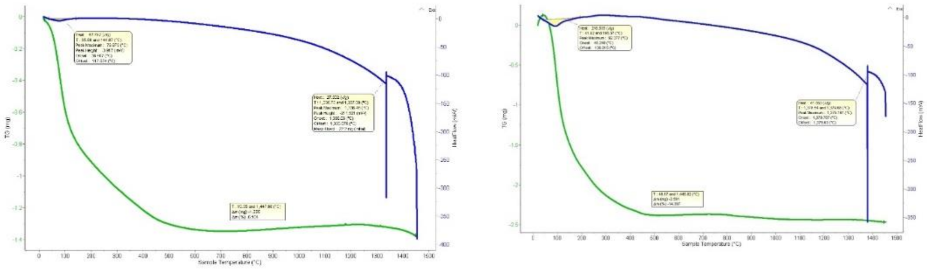

a) b)

Figure 4. 6. DSC-TG analysis for a) ZrO2CeRO powder and b) ZrO2RE powder.

DSC-TG measurements for both types of powders are similar to powders doped with a single REO element. Thus, a continuous mass loss up to about 500 °C and an endothermic peak around 70 for ZrO2CeRO powder and around 90 for ZrO2RE powder are observed. The latter are attributed to a dehydration process of the materials, which is in agreement with other studies in the literature..

Thermal analysis

The thermal conductivity values obtained for the P5-ZrO2RE and P6-ZrO2CeRO samples are 0.8902 ± 0.00311 and 0.68228 ± 0.0035, respectively.

CHAPTER V. EXPERIMENTAL RESEARCH ON THE OBTAINING AND CHARACTERIZATION OF THERMAL BARRIERS

5.1 Obtaining thermal barriers based on ZrO_2 doped with REO

In this chapter, it was aimed to obtain two types of thermal barriers based on ZrO2RE and ZrO2CeRO powders. The architecture of the two types of TBC developed by the EB-PVD technique is presented in figure 5.1.

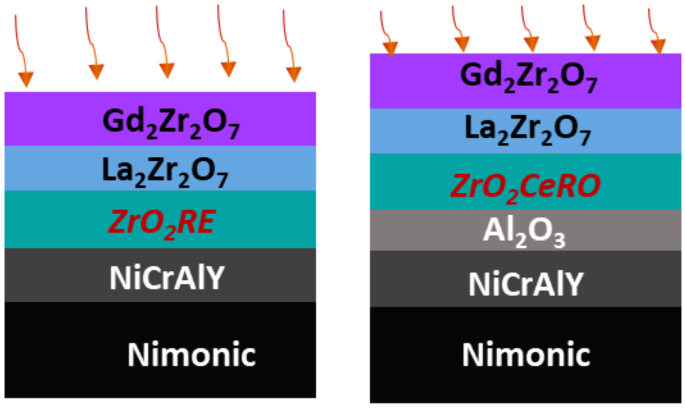

Figure 5. 1 The architecture of the thermal barriers developed in this study.

These TBCs were developed in a special EB-PVD thin film coating equipment (Torr International Inc., New Windsor, NY, USA – Figure 5.3) equipped with quartz sensors (QCM) mounted next to each crucible to monitor deposition rate and software that allows the creation of a complex deposition recipe that can be performed automatically while keeping the evaporation rate constant.

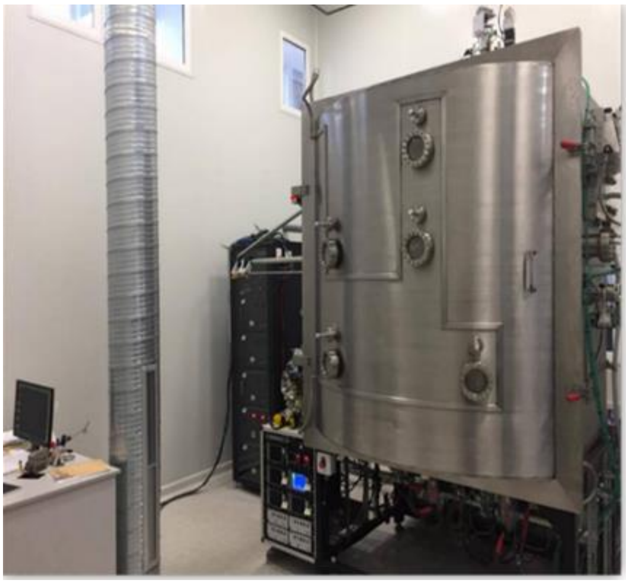

Figure 5. 2. EB-PVD system.

All successive layers were deposited by the EB-PVD process. Commercial NiCrAlY powders (Amperit) were used to deposit the acros layer before the ceramic layer was deposited. Commercial

$La_2Zr_2O_7$ (LZO) granulated powders (30−120 μm grain sizes) and $Gd_2Zr_2O_7$ (GZO) granulated powders (45−140 μm grain sizes) from Trans-Tech Ceramics and Advanced Materials USA were also used for to deposit the outer layers, aiming to improve the thermal shock properties of the system.

To ensure a gradual transition from the composition of the Al_2O_3 layer to that of LZO, ZrO2 powders co-doped with a mixture of rare earths, ZrO2RE and ZrO2CeRO obtained by a hydrothermal technology were used for the first time. At the same time, the selection of this material corresponds to the trends in the specialized literature for obtaining composite materials with improved mechanical properties.

5.2 Characterization of thermal barriers based on ZrO_2 doped with REO

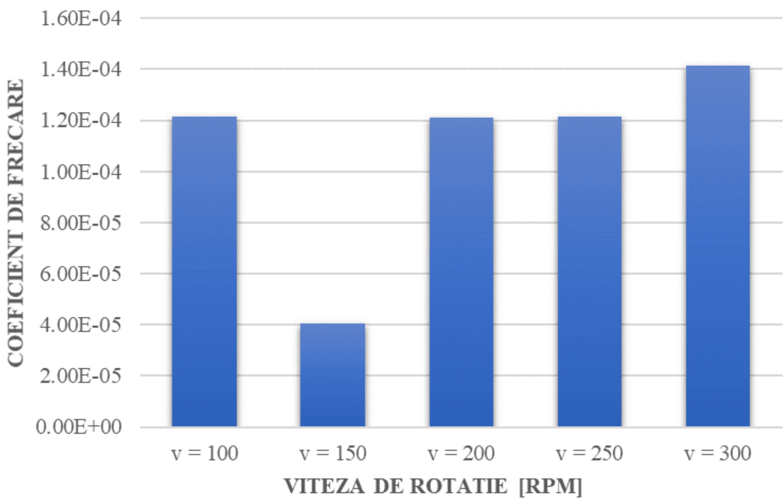

Figura 5. 3. Mass wear rate values for the tested specimens.

From the wear rate analysis (Figure 5. 9), for Nimonic + NiCrAlY/Al_2O_3/ZrO2CeRO/La2Zr2O7/Gd2Zr2O7 samples, the lowest value was obtained at the sliding speed of 150 rpm, and the highest wear rate is given by testing the sample at a speed of 300 rpm. For the rest of the test speeds, the wear rate is about the same value.

SEM analysis

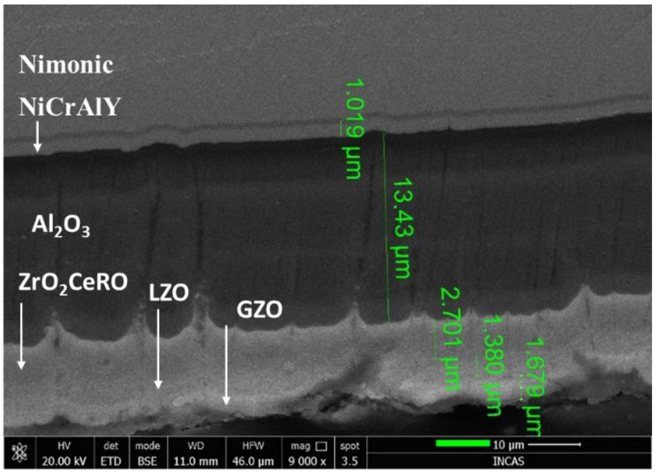

Figura 5. 4. SEM image in section for Nimonic+ sample NiCrAlY/Al_2O_3/ ZrO2CeRO/ LZO/ GZO.

As can be seen in the image, the coating shows a columnar structure, with grains perpendicular to the surface, which is a typical characteristic of EB-PVD coating, care este o caracteristică tipică a acoperirii EB-PVD [194,195].

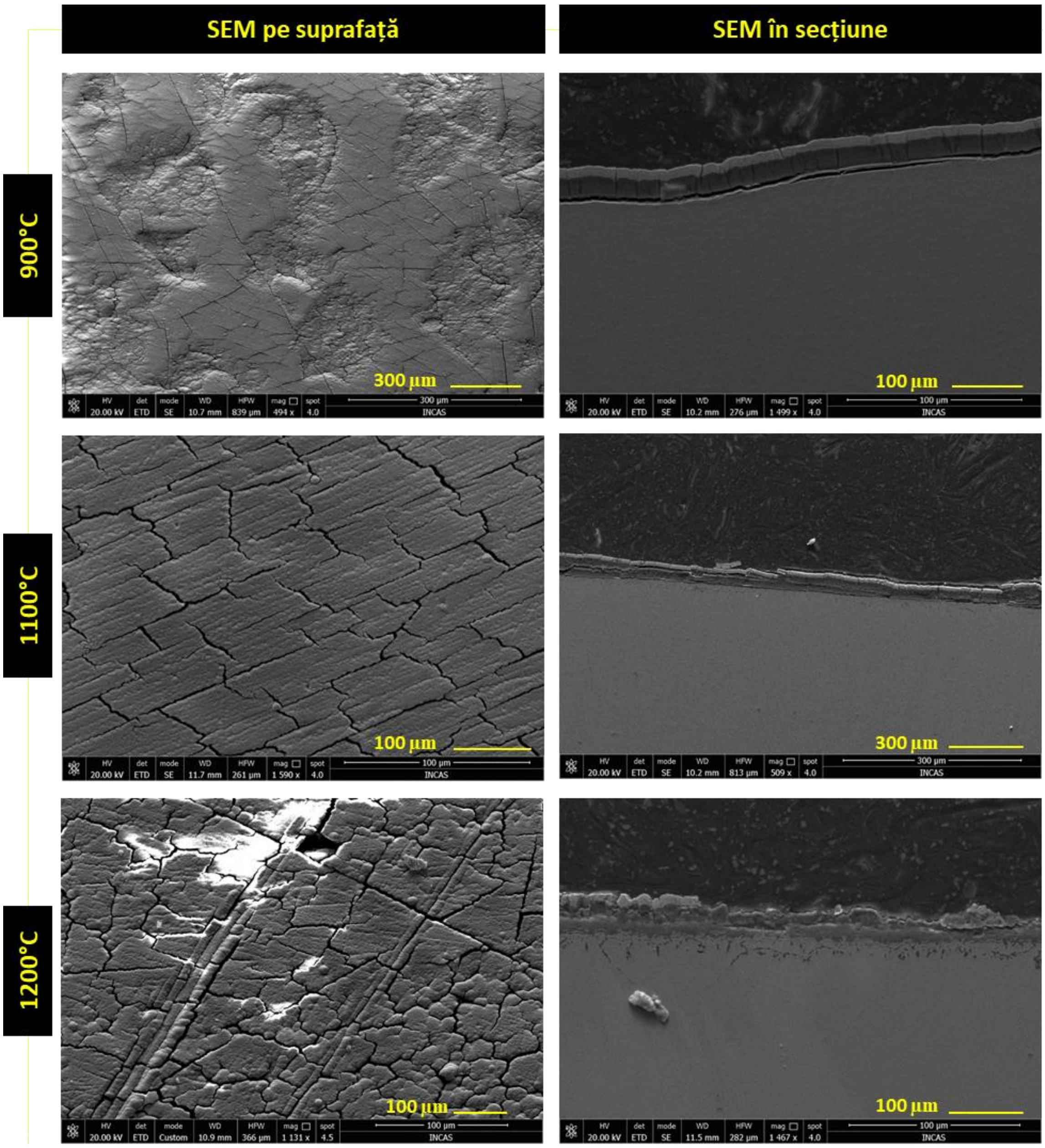

Figure 5.12 studies the surface and cross-sectional microstructure of ZrO2CeRO-based TBCs after thermal shock testing at different temperatures.

At the temperature of 1200 °C, the thermal barrier layer suffers the greatest destruction, compared to the other samples.

Increased vertical cracks at the interface contribute to providing the heat flow channel, therefore the bonding layer experiences higher temperature oxidation during thermal shock tests [196].

The exfoliation of the surface layer can be attributed to the high level of internal stresses that occur at the interface between the layers.

5.2.3. Characterization of thermal barriers based on ZrO2RE

DRX analysis

The Nimonic sample with 4 layers of NiCrAlY/YSZ/LZO/GZO type material was subjected to heat treatment at a temperature of 1250°C for 10 minutes in nitrogen to determine its behavior under high temperature conditions.

The diffractogram obtained for the Nimonic support covered with 4 layers of material (NiCrAlY/YSZ/LZO/GZO) after thermal treatment (figure 5.18) shows the phases $Gd_2Zr_2O_7$ (ICDD PDF4+ 01-078-4083) and $La_2Zr_2O_7$ (ICDD PDF4+ 00-050-0837) characteristic of the last 2 layers deposited on the Nimonic support

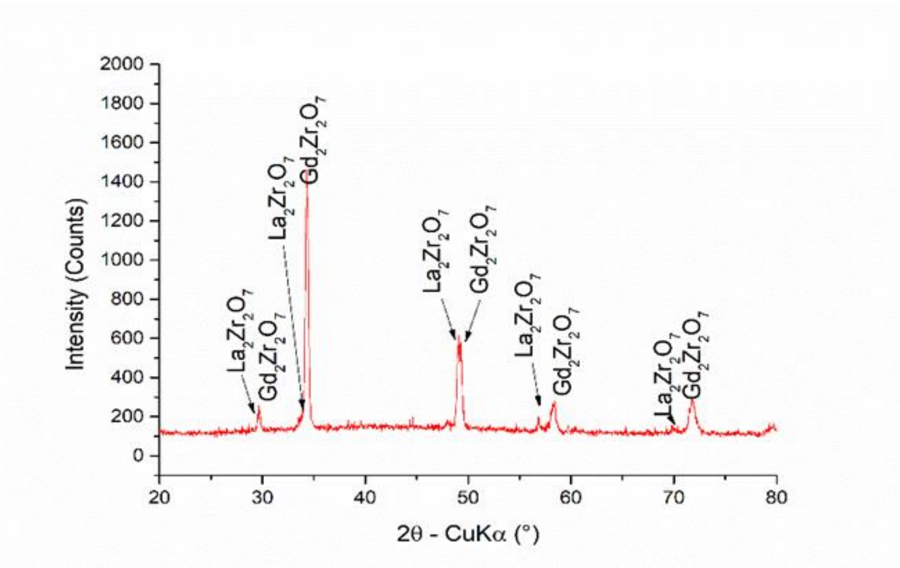

Figura 5. 14. X-ray diffraction spectrum obtained for Nimonic with 4 material layers (NiCrAlY/YSZ/LZO/GZO) after heat treatment at 1250°C.

SEM analysis

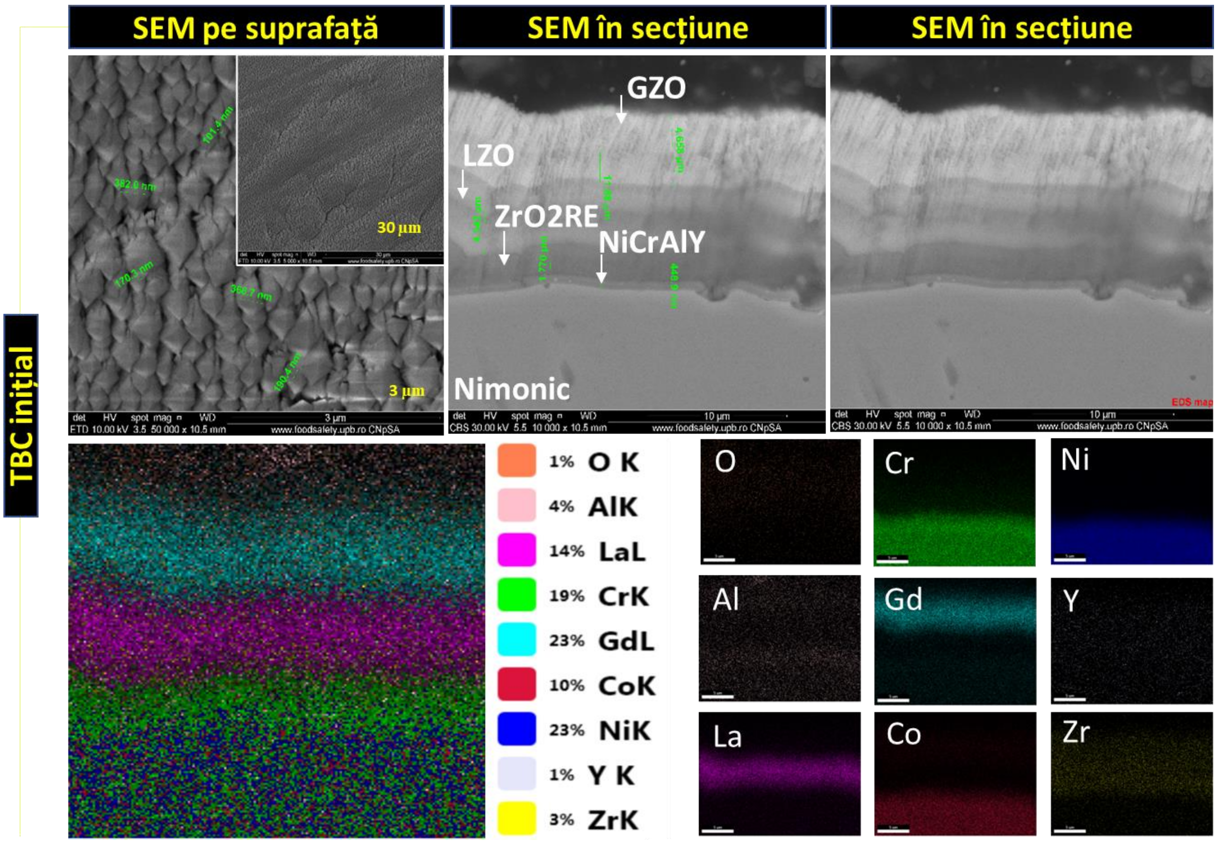

Figura 5. 5. SEM images at different magnifications (x5,000, x50,000), representing the surface of NiCrAlY/ZrO2RE/LZO/GZO type deposition on Nimonic substrate, the cross-sectional view of NiCrAlY/YSZ/LZO/GZO type deposition on Nimonic substrate, as well and elemental mapping.

The SEM analysis on the surface of the Nimonic sample with 4 layers of material (NiCrAlY/YSZ/LZO/GZO) (figure 5.15) shows that the deposition is uniform and a continuous film is present on the support. Polyhedral granules with well-defined edges and sizes between 190 and 380 nm are identified.

The sectional view of the Nimonic support with NiCrAlY/YSZ/LZO/GZO type coatings highlights the presence of the 4 layers arranged as follows: NiCrAlY with a layer thickness of 448.9 nm, YSZ with a layer thickness of 1,770 µm, LZO with a layer thickness of 4,543 µm and GZO with layer thickness of 4,658 µm. The total thickness of the deposit having a size of 12.15 µm. The elemental mapping delimits through the chosen colors the specific elements of the layout of the coverage in the form of multilayers.

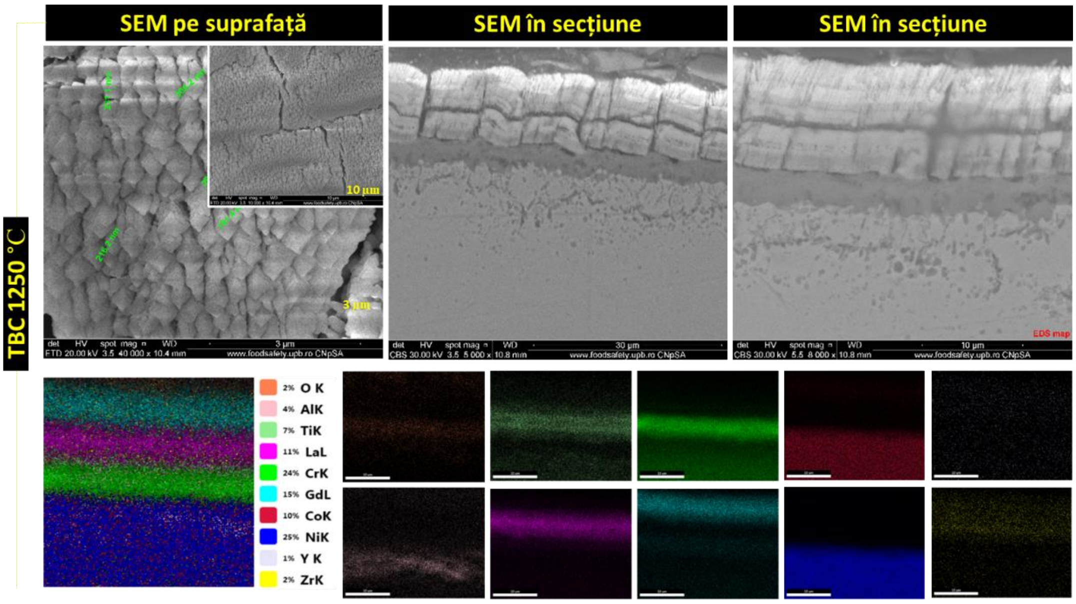

Figura 5. 6. SEM images at different magnifications (x5,000, x50,000), representing the surface of the NiCrAlY/ZrO2RE/LZO/GZO type deposition on Nimonic substrate, the sectional view of the NiCrAlY/ZrO2RE/LZO/GZO type deposition on Nimonic substrate, as well and elemental mapping at a temperature of 1250°C.

In the SEM micrographs obtained after the treatment, it can be seen that the layers did not change their morphology, being similar to the sample before the heat treatment. The film is uniform on the substrate, but cracks appear at the intergranular boundaries.

After the thermal treatment, the cross-sectional view of the Nimonic sample with 4 layers of NiCrAlY/ZrO2RE/LZO/GZO material and the elemental mapping leads to the following conclusions: the thermal shock caused the cracking of the ZrO2RE layer, the diffusion of Ti to the contact layer and Cr from the contact to the substrate as well as the formation of TiO_2.

Roughness

From the results of the roughness investigations shown in Figure 5.17, a slight change in the average surface roughness can be observed from 0.448 µm of the Nimonic 80A substrate to 0.521 µm for the coated Nimonic substrate. These values are very similar, thus proving that the coatings grow uniformly following the substrate morphology.

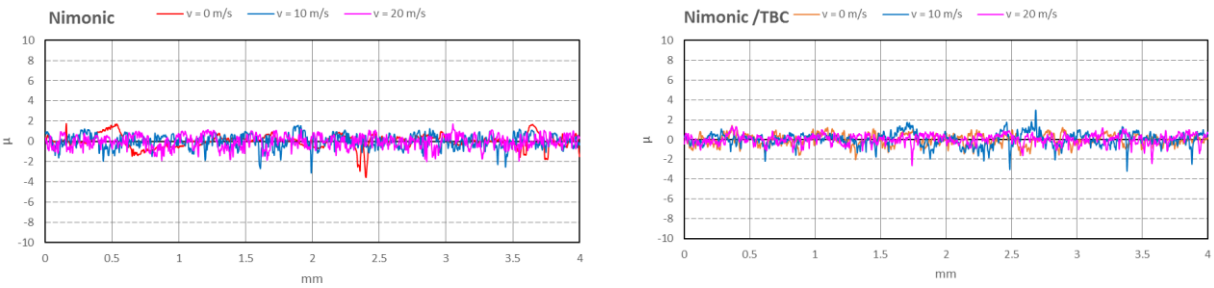

Figure 5. 7. Surface roughness studies of uncoated and coated Nimonic 80A substrate.

Thermal shock

The results of the thermal shock tests are shown in Figure 5.18 and Figure 5.19. This test shows the number of heating and cooling cycles that a coated material can withstand without delamination of the coating layers. The comparison of the thermal shock values of the new coatings architecture with the existing ones can be a method to evaluate their potential application in aeronautics. The results show a satisfactory behavior obtained after a minimum number of 150 cycles in the temperature ranges 1200-1300 °C for the proposed NiCrAlY/ZrO2-RE1/LZO/GZO coating architecture with a total thickness of about 11.5 µm. The results are comparable to those of traditional YSZ coatings with thickness greater than 100 µm [65], showing the ability of the new coating materials to further improve the thermal properties of TBCs at much lower thickness.

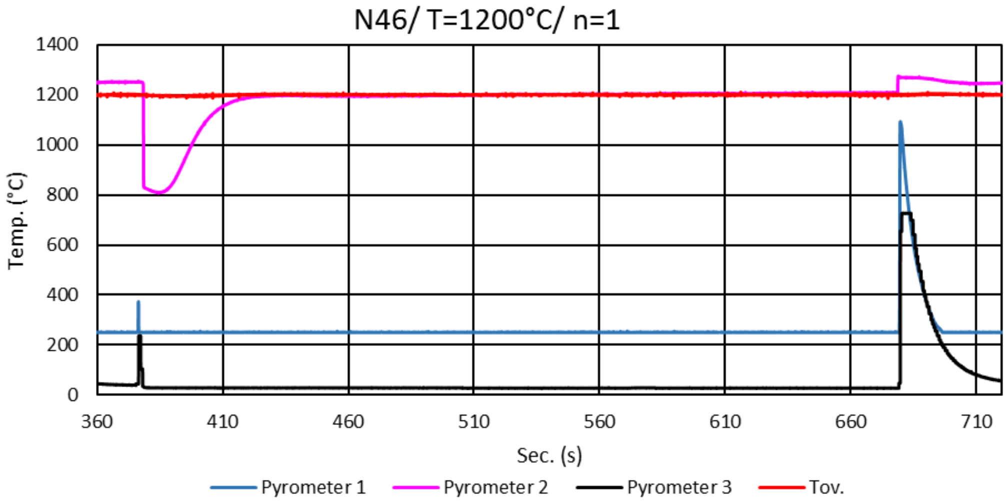

Figura 5. 8. Thermal shock tests. Red line (TCup)—represents the furnace temperature recorded by the Pt/PtRh thermocouple mounted inside the furnace; the magenta line (pyrometer 2) represents the temperature of the sample over the heating stage during the test, which shows a peak starting from the low temperature and a stabilized temperature for the waiting time. The blue and black lines represent the sample temperature change in the cooling step by pyrometer 1 and pyrometer 3, respectively.

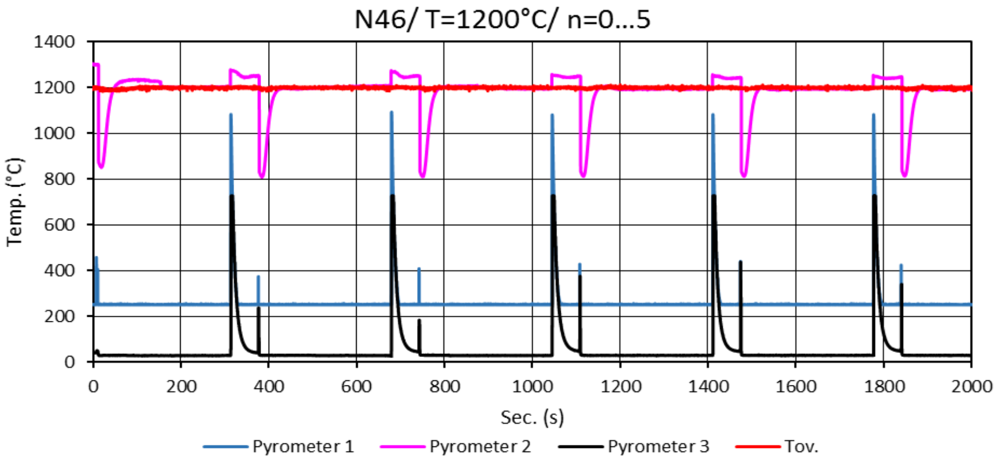

Figura 5. 9. Thermogram for thermal shock cycles 38–43, temperature range 800–1300 °C.

CHAPTER VI. DEVELOPMENT OF A MARKET STUDY REGARDING THERMAL BARRIERS

This section will help to establish an overview of the industrial development and characteristics of the Thermal Barrier Coatings market. This study is based on data provided by Maya Research Analysis, where 2016 is considered a historical year, 2020 a base year, 2021 an estimated year and 2027 a forecast year. The study is segmented by market analysis based on type of materials used, applications, region and TBC manufacturing companies.

According to the research, the global thermal barrier coatings market has a total sales value of USD 697.07 million in 2016 and will grow to USD 1990.43 million in 2020. TBC markets forecast may be USD 2827.82 million by 2027 .The TB CAGR is 6.03% from 2021 to 2027.

North America was the largest revenue market with a market share of 41.91% in 2016 and 41.77% in 2021, a decrease of 0.14%. Europe ranked second with a market share of 35.68% in 2020. Also, the Asia Pacific market for thermal barrier coatings is expected to be the market with the most promising growth rate. The development of the economy, the progress of technological innovation in the emerging economies, specifically in China and India, have led to an increase in demand.

Thermal barrier coating companies are mainly from the US and Europe; the concentration rate of the industry is relatively low. The top three companies are Praxair Surface Technologies, Cincinnati Thermal Spray and Treibacher Industrie AG with a revenue market share of 9.17%, 6.67% and 6.14% in 2020.

The global thermal barrier coatings market is expected to witness growth during the forecast period due to multiple demands from downstream industries. The other factor driving the growth of the thermal barrier coatings market is continuous innovation.

CONCLUSIONS, PERSONAL CONTRIBUTIONS AND RESEARCH DIRECTIONS..

Final conclusions

The doctoral thesis with the theme *Research on the effective use of critical raw materials as dopants in zirconium-based materials for applications in extreme conditions*, was based on the extensive study of specialized literature that concluded several aspects related to the current trends in the field of interest as follows:

- Critical raw materials form a strong industrial base that contributes to the production of a wide range of products and applications used in everyday life and in modern technologies. They enable European industry to meet the EU's political objectives. A first EU assessment of critical raw materials was launched in 2008. A priority action was the establishment of an EU-wide list of critical raw materials in 2011. This list was a response to the challenges related to their economic importance and their risk of supply and is updated every three years to regularly assess the criticality of raw materials.

- Among the critical raw materials at the European level are REE. The need for increased and sustained action was emphasized so that their use as critical raw materials is more sustainable and with a low environmental impact.

- The most widely used ceramic material for thermal barriers is zirconia stabilized with 7-8% yttrium (YSZ), which is otherwise considered to be the gold standard for TBC for turbines;

- However, the main disadvantage of YSZ is actually its stability above 1200 °C, due to the phase transformation with increasing volume upon long-term exposure (generally greater than 100 h) at high temperatures. Moreover, after prolonged exposure to high temperatures, YSZ tends to sinter and/or increase its thermal conductivity and is also susceptible to infiltration of CMAS (calcium magnesium aluminum silicates). Therefore, the development of new TBC materials that can be applied at high temperatures for a long time is urgently needed;

- Zirconia with the non-transformable tetragonal (t') phase was found to be harder than the cubic phase due to ferroelastic hardening;

- In recent years, there is an increasing theoretical and practical interest in the use of various REO mixtures as dopants for high-temperature ceramics, especially for ZrO_2-based thermal barrier coatings (TBCs) used in aeronautics and co - energy generation;

- It has been reported that by co-doping zirconia with different REOs to improve the thermal properties of thermal barrier coatings and the oxidation properties, due to the reduction of mechanical stresses and porosity in the oxide layers;

- Several studies have shown that the structure of multilayer TBCs exhibits better properties compared to single-layer TBCs. As a rule, the lower layer is YSZ, and the upper layer should be a material with high temperature phase stability. Such types of materials are pyrochlore and perovskite.

Taking this information into account, **the objectives, research methodology and work plan were formulated.**

In the present thesis, the strategy of using mixed REOs instead of individual REOs was adopted in order to minimize the environmental impact and decrease the production costs of potential applications.

The main objective of the doctoral thesis was achieved by::

- The development by the hydrothermal method of two types of materials based on a synthetic mixture of rare earth oxides: MxZyCeRO and MxZyRE. The basis for obtaining these powders was an experimental study related to the doping of zirconia with different amounts (4, 6, 8% by weight) of individual REO elements (La, Nd, Sm, Gd) in order to follow the influence of each element in what concerns structure and morphology;

- The development by the EB-PVD method of two categories of TBCs with several layers, among which ZrO_2 doped with rare earths as an intermediate layer between the bonding layer and the LZ, with the aim of adjusting the thermal mismatch, as well as improving the cycle execution thermal of TBC.

The results of the research activities carried out indicated:

- The efficiency of using hydrothermal synthesis in obtaining ceramic materials based on ZrO2 doped with a synthetic mixture of rare earths.

Thus, a number of 12 powders were obtained, ZrO_2 doped with 8% Y_2O_3 and co-doped with 4/6/8% RE unitary dopant (La, Nd, Sm, Gd), for which the phase evolution was followed and the morphology of the powders at different heat treatment temperatures.

S-au obținut pulberi nanocristaline formate din ZrO_2 cu structură cubică drept fază majoră și M-ZrO_2 obtained nanocrystalline powders consisting of cubic ZrO_2 as the major phase and monoclinic M-ZrO2 (Baddeleyite) as the secondary phase, except for Nd-doped YSZ which consisted of only a cubic phase. The phase evolution of the powders during heat treatment in the range 400–1400 °C shows the progressive formation of different solid solutions through the isomorphous replacement of Zr^{4+} by Ln^{3+} It was found that the optimal heat treatment temperature is 1200 °C, where the formation of pyrochlore solid solutions (Pyr-$RE_2Zr_2O_7$ where RE—Y and Ln) is observed for all compositions, except for samples co-doped with 4, 6 and 8 wt % Nd, 6 and 8 wt % Sm and 8 wt % Gd, when only the cubic phase was observed (ZrO_2) SS- ($Ln_{0,14}$ $Y_{0,14}$ $Zr_{0,72}$) $O_{1,86}$.

Low values of thermal conductivities were measured by the hot plate method at room temperature.

Both ZrO2RE and ZrO2CeRO powders obtained by hydrothermal synthesis showed tetragonal structure. The ZrO2CeRO sample presented, instead, a monoclinic phase as the secondary phase.

- The feasibility of making thermal barrier type coatings that include ZrO_2 doped with a synthetic mixture of rare earths as an intermediate layer between the acros and the surface substrates. Two types of thermal barriers were obtained::

In the case of the uncoated NIMONIC 80 substrate, which was subjected to heat treatment at 1250 °C, a change in the surface morphology and an appearance of oxidation as a result of the temperature to which it was subjected, was observed, through the appearance of TiO_2 and Cr_2O_3.

Structural and morphological analysis confirmed that multilayer TBCs were successfully obtained. Thus, the microstructure of both types of coatings indicates that through the EB-PVD technique, coatings with uniform, dense structures were obtained, with a columnar structure and grains perpendicular to the surface, a characteristic structure of this deposition technique.

In the case of TBCs with the NiCrAlY/ ZrO2RE/La2Zr2O7/Gd2Zr2O architecture, which was subjected to heat treatment at 1250 °C for 10 minutes, in nitrogen it was observed that no significant change in morphology occurred, cracks appearing at the intergranular boundary , but without affecting the substrate. The roughness study on both the simple substrate and the one deposited with the architecture... proved the fact that the coatings grow uniformly, following the morphology of the substrate.

The results of the thermal shock tests on this architecture, after a number of more than 150 cycles at the temperature between 1200-1300 °C, are comparable to those of the classic YSZ coatings that have a much greater thickness. Thus, the capacity of these new types of coatings is highlighted, for the development of TBCs with a much smaller thickness, thus reducing the consumption of critical raw materials.

For TBC with the NiCrAlY/Al_2O_3/ZrO2CeRO/La2Zr2O7/Gd2Zr2O architecture, analyzing the surface of the samples after thermal shock testing at different temperatures, total cycles 0-50, it was found that a partial exfoliation of the upper layer occurs at a temperature of 1200, which can be due to the high level of internal stresses that occur at the interface between the metal layer (Bond Coat -BC) and that of the overlays of oxide layers (Al_2O_3/ ZrO2CeRO/ La2Zr2O7/ Gd2Zr2O7) chosen for the system the upper ceramic layer of the thermal barrier (Top Coat). Although this partial exfoliation occurs, no changes are evident at the substrate level, showing potential for applications such as thermal barriers.

Therefore, the results concluded above, underline the fact that the use of ZrO_2 doped with mixed rare earths, combined with pyrochlore-type materials (LZO, GZO) in the architecture of TBCs leads to obtaining thermal barriers with a reduced content of critical raw materials, which have properties similar to those currently used.

Original contribution

Original contributions were made at each stage, from the literature study, to the choice of dopants, the design of ceramic powders and thermal barriers, to the selection of technological process parameters..

Below are the original contributions, described extensively throughout the doctoral thesis:

- Carrying out a **specialized literature study** on the areas of interest: critical raw materials and strategic technologies, rare earth elements and their applications, obtaining ceramic materials based on rare earths, obtaining TBC based on rare earths;

- Realization of some **thermodynamic predictions** of hydrothermal reactions to obtain ceramic materials based on ZrO_2 doped with rare earths;

- The study of the influence of different amounts of e REE (La, Nd, Sm and Gd) used as co-dopants on the morphology and structure of zirconium doped with 8% by weight Y_2O_3 was carried out;

- Demonstration of the potential of using the synthetic mixed mixture of REO to obtain two types of ZrO2-based materials in the form of powders (ZrO2RE, ZrO2CeRO) with promising properties related to the use for the development of thermal barriers. Achieving such results is an important milestone.

- Demonstration of the potential of using the synthetic mixed mixture of REO to obtain two types of thermal barriers;

- Carrying out a market study on TBC.

Perspectives of further research

- The development of ceramic materials based on ZrO_2 doped with a natural mixture of rare earths;
- Development of TBCs based on ZrO_2 doped with a natural mixture of rare earths;
- Development of REE-doped ZrO_2 thin films for applications in solid oxide fuel cells.

BIBLIOGRAFIE

1. Ferro, P.; Bonollo, F. Design for Recycling in a Critical Raw Materials Perspective. Recycling 2019, 4, doi:10.3390/recycling4040044.

2. Hofmann, M.; Hofmann, H.; Hagelüken, C.; Hool, A. Critical Raw Materials: A Perspective from the Materials Science Community. Sustain. Mater. Technol. 2018, 17, e00074, doi:10.1016/j.susmat.2018.e00074.

3. Martins, F.; Castro, H. Significance Ranking Method Applied to Some EU Critical Raw Materials in a Circular Economy – Priorities for Achieving Sustainability. Procedia CIRP 2019, 84, 1059–1062, doi:10.1016/j.procir.2019.04.281.

4. Kim, J.; Lee, J.; Kim, B.C.; Kim, J. Raw Material Criticality Assessment with Weighted Indicators: An Application of Fuzzy Analytic Hierarchy Process. Resour. Policy 2019, 60, 225–233, doi:10.1016/j.resourpol.2019.01.005.

7. Andersson, P. Chinese Assessments of “Critical” and “Strategic” Raw Materials: Concepts, Categories, Policies, and Implications. Extr. Ind. Soc. 2020, 7, 127–137, doi:10.1016/j.exis.2020.01.008.

10. Hayes, S.M.; McCullough, E.A. Critical Minerals: A Review of Elemental Trends in Comprehensive Criticality Studies. Resour. Policy 2018, 59, 192–199, doi:10.1016/J.RESOURPOL.2018.06.015.

11. Achzet, B.; Helbig, C. How to Evaluate Raw Material Supply Risks—an Overview. Resour. Policy 2013, 38, 435–447, doi:10.1016/J.RESOURPOL.2013.06.003.

20. Regiunilor, C. Pactul Ecologic European (European Green Deal).Pdf. 2019.

21. 6 Strategia Industriala.

22. The Raw Materials Initiative-Meeting Our Critical Needs for Growth and Jobs in Europe. 2008.

23. European Commission Study on the Critical Raw Materials for the EU; 2023; ISBN 9789268004135.

25. Dewulf, J.; Blengini, G.A.; Pennington, D.; Nuss, P.; Nassar, N.T. Criticality on the International Scene: Quo Vadis? Resour. Policy 2016, 50, 169–176, doi:10.1016/j.resourpol.2016.09.008.

26. Rabe, W.; Kostka, G.; Smith Stegen, K. China’s Supply of Critical Raw Materials: Risks for Europe’s Solar and Wind Industries? Energy Policy 2017, 101, 692–699, doi:10.1016/j.enpol.2016.09.019.

27. Security of Supply for Critical Raw Materials Vulnerabilities and Areas for G7 Coordination.

28. Bobba, S.; Carrara, S.; Huisman, J.; Mathieux, F.; Pavel, C. Critical Raw Materials for Strategic Technologies and Sectors in the EU - a Foresight Study; 2020; ISBN 9789276153375.

66. Balaram, V. Rare Earth Elements: A Review of Applications, Occurrence, Exploration, Analysis, Recycling, and Environmental Impact. Geosci. Front. 2019, 10, 1285–1303, doi:10.1016/J.GSF.2018.12.005.

79. Piticescu, R.R.; Slobozeanu, A.E.; Valsan, S.N.; Ciobota, C.F.; Ghita, A.N.; Motoc, A.M.; Chiriac, S.; Prakasam, M. Hydrothermal Synthesis of Nanocrystalline ZrO2-8Y2O3-XLn2O3 Powders (Ln = La, Gd, Nd, Sm): Crystalline Structure, Thermal and Dielectric Properties. Mater. 2021, Vol. 14, Page 7432 2021, 14, 7432, doi:10.3390/MA14237432.

82. Why Processing Sweden's Rare-Earth Haul Won't Be Easy Available online: https://www.wsj.com/articles/why-processing-swedens-rare-earth-haul-wont-be-easy-11675935006 (accessed on 1 March 2023).

87. Kisi, E.H.; Howard, C.J. Crystal Structures of Zirconia Phases and Their Inter-Relation. Key Eng. Mater. 1998, 153–154, 1–36, doi:10.4028/WWW.SCIENTIFIC.NET/KEM.153-154.1.

88. Idrissi, S.; Ziti, S.; Labrim, H.; Bahmad, L. Sulfur Doping Effect on the Electronic Properties of Zirconium Dioxide ZrO2. Mater. Sci. Eng. B 2021, 270, 115200, doi:10.1016/J.MSEB.2021.115200.

89. Madhusudhana, H.C.; Shobhadevi, S.N.; Nagabhushana, B.M.; Hari Krishna, R.; Murugendrappa, M.V.; Nagabhushana, H. Structural Characterization and Dielectric Studies of Gd Doped ZrO2 Nano Crystals Synthesized by Solution Combustion Method. Mater. Today Proc. 2018, 5, 21195–21204, doi:10.1016/J.MATPR.2018.06.519.

90. Fan, W.; Bai, Y.; Wang, Y.; He, T.; Gao, Y.; Zhang, Y.; Zhong, X.; Li, B.; Chang, Z.; Ma, Y. Microstructural Design and Thermal Cycling Performance of a Novel Layer-Gradient Nanostructured Sc2O3–Y2O3 Co-Stabilized ZrO2 Thermal Barrier Coating. J. Alloys Compd. 2020, 829, 154525, doi:10.1016/J.JALLCOM.2020.154525.

91. Hao, S.J.; Wang, C.; Liu, T. Le; Mao, Z.M.; Mao, Z.Q.; Wang, J.L. Fabrication of Nanoscale Yttria Stabilized Zirconia for Solid Oxide Fuel Cell. Int. J. Hydrogen Energy 2017, 42, 29949–29959, doi:10.1016/J.IJHYDENE.2017.08.143.

92. Miura, N.; Sato, T.; Anggraini, S.A.; Ikeda, H.; Zhuiykov, S. A Review of Mixed-Potential Type Zirconia-Based Gas Sensors. Ionics (Kiel). 2014, 20, 901–925, doi:10.1007/S11581-014-1140-1/FIGURES/27.

93. Kauppi, E.I.; Honkala, K.; Krause, A.O.I.; Kanervo, J.M.; Lefferts, L. ZrO2 Acting as a Redox Catalyst. Top. Catal. 2016, 59, 823–832, doi:10.1007/S11244-016-0556-4/FIGURES/7.

94. Savin, A.; Craus, M.L.; Turchenko, V.; Bruma, A.; Dubos, P.A.; Malo, S.; Konstantinova,

T.E.; Burkhovetsky, V. V. Monitoring Techniques of Cerium Stabilized Zirconia for Medical Prosthesis. Appl. Sci. 2015, Vol. 5, Pages 1665-1682 2015, 5, 1665–1682, doi:10.3390/APP5041665.

95. Huang, R.; Yan, X.; Ye, S.; Kashtiban, R.; Beanland, R.; Morgan, K.A.; Charlton, M.D.B.; de Groot, C.H. Compliance-Free ZrO2/ZrO2 − x/ZrO2 Resistive Memory with Controllable Interfacial Multistate Switching Behaviour. Nanoscale Res. Lett. 2017, 12, doi:10.1186/s11671-017-2155-0.

96. Saridag, S.; Tak, O.; Alniacik, G. Basic Properties and Types of Zirconia: An Overview. http://www.wjgnet.com/ 2013, 2, 40–47, doi:10.5321/WJS.V2.I3.40.

97. The Secrets of Zirconia Ceramic Bearings, Toughness Available online: https://www.lyrabearing.com/en/blog/secrets-of-zirconia-ceramic-bearings-toughness (accessed on 15 March 2023).

98. Bahamirian, M.; Hadavi, S.M.M.; Farvizi, M.; Rahimipour, M.R.; Keyvani, A. Phase Stability of ZrO2 9.5Y2O3 5.6Yb2O3 5.2Gd2O3 Compound at 1100 °C and 1300 °C for Advanced TBC Applications. Ceram. Int. 2019, 45, 7344–7350, doi:10.1016/J.CERAMINT.2019.01.018.

99. Zakaria, Z.; Abu Hassan, S.H.; Shaari, N.; Yahaya, A.Z.; Boon Kar, Y. A Review on Recent Status and Challenges of Yttria Stabilized Zirconia Modification to Lowering the Temperature of Solid Oxide Fuel Cells Operation. Int. J. Energy Res. 2020, 44, 631–650, doi:10.1002/ER.4944.

100. Ali, S.A.; Karthigeyan, S.; Deivanai, M.; Ma, R. Ziconia: Porperties and Application — A Review. Pakistan Oral Dent. J 2014, 34, 178–183.

103. Mikhailov, D.A.; Orlova, A.I.; Malanina, N. V.; Nokhrin, A. V.; Potanina, E.A.; Chuvil'deev, V.N.; Boldin, M.S.; Sakharov, N. V.; Belkin, O.A.; Kalenova, M.Y.; et al. A Study of Fine-Grained Ceramics Based on Complex Oxides ZrO2-Ln2O3 (Ln = Sm, Yb) Obtained by Spark Plasma Sintering for Inert Matrix Fuel. Ceram. Int. 2018, 44, 18595–18608, doi:10.1016/J.CERAMINT.2018.07.084.

110. Prakasam, M.; Valsan, S.; Lu, Y.; Balima, F.; WenzhongLu; Piticescu, R.; Largeteau, A.; Prakasam, M.; Valsan, S.; Lu, Y.; et al. Nanostructured Pure and Doped Zirconia: Synthesis and Sintering for SOFC and Optical Applications. Sinter. Technol. - Method Appl. 2018, doi:10.5772/INTECHOPEN.81323.

111. Sasikumar, K.; Bharathikannan, R.; Raja, M.; Mohanbabu, B. Fabrication and Characterization of Rare Earth (Ce, Gd, and Y) Doped ZrO2 Based Metal-Insulator-Semiconductor (MIS) Type Schottky Barrier Diodes. Superlattices Microstruct. 2020, 139, 106424, doi:10.1016/J.SPMI.2020.106424.

112. Mekala, R.; Deepa, B.; Rajendran, V. Preparation, Characterization and Antibacterial Property of Rare Earth (Dy and Ce) Doping on ZrO2 Nanoparticles Prepared by Co-Precipitation Method. Mater. Today Proc. 2018, 5, 8837–8843, doi:10.1016/J.MATPR.2017.12.315.

144

113. Guo, L.; Li, M.; Ye, F. Phase Stability and Thermal Conductivity of RE2O3 (RE=La, Nd, Gd, Yb) and Yb2O3 Co-Doped Y2O3 Stabilized ZrO2 Ceramics. Ceram. Int. 2016, 42, 7360–7365, doi:10.1016/J.CERAMINT.2016.01.138.

114. Chen, C.; Liang, T.; Guo, Y.; Chen, X.; Man, Q.; Zhang, X.; Zeng, J.; Ji, V. Effect of Scandia Content on the Hot Corrosion Behavior of Sc2O3 and Y2O3 Co-Doped ZrO2 in Na2SO4 + V2O5 Molten Salts at 1000 °C. Corros. Sci. 2019, 158, 108094, doi:10.1016/J.CORSCI.2019.108094.

115. Song, X.; Xie, M.; Mu, R.; Zhou, F.; Jia, G.; An, S. Influence of the Partial Substitution of Y2O3 with Ln2O3 (Ln = Nd, Sm, Gd) on the Phase Structure and Thermophysical Properties of ZrO2–Nb2O5–Y2O3 Ceramics. Acta Mater. 2011, 59, 3895–3902, doi:10.1016/J.ACTAMAT.2011.03.014.

116. Wang, Y.T.; Chen, L.; Feng, J. Impact of ZrO2 Alloying on Thermo-Mechanical Properties of Gd3NbO7. Ceram. Int. 2020, 46, 6174–6181, doi:10.1016/J.CERAMINT.2019.11.084.

117. Song, X.; Xie, M.; An, S.; Hao, X.; Mu, R. Structure and Thermal Properties of ZrO2–Ta2O5–Y2O3–Ln2O3 (Ln = Nd, Sm or Gd) Ceramics for Thermal Barrier Coatings. Scr. Mater. 2010, 62, 879–882, doi:10.1016/J.SCRIPTAMAT.2010.02.033.

119. Salman, S.; Köse, R.; Urtekin, L.; Findik, F. An Investigation of Different Ceramic Coating Thermal Properties. Mater. Des. 2006, 27, 585–590, doi:10.1016/J.MATDES.2004.12.010.

120. Gautam, S.S.; Singh, R.; Vibhuti, A.S.; Sangwan, G.; Mahanta, T.K.; Gobinath, N.; Feroskhan, M. Thermal Barrier Coatings for Internal Combustion Engines: A Review. Mater. Today Proc. 2022, 51, 1554–1560, doi:10.1016/J.MATPR.2021.10.371.

121. Shrirao, P.N.; Pawar, A.N. Evaluation of Performance and Emission Characteristics of Turbocharged Diesel Engine with Mullite as Thermal Barrier Coating. Int. J. Eng. Technol. 2011, 3, 256–262.

122. Zhu, D.; Miller, R.A.; Fox, D.S. Thermal and Environmental Barrier Coating Development for Advanced Propulsion Engine Systems. Collect. Tech. Pap. - AIAA/ASME/ASCE/AHS/ASC Struct. Struct. Dyn. Mater. Conf. 2007, 5, 5121–5135, doi:10.2514/6.2007-2130.

123. Selvam, M.; Shanmugan, S.; Palani, S. Performance Analysis of IC Engine with Ceramic-Coated Piston. Environ. Sci. Pollut. Res. 2018, 25, 35210–35220, doi:10.1007/S11356-018-3419-7/METRICS.

124. Dhomne, S.; Mahalle, A.M. Thermal Barrier Coating Materials for SI Engine. J. Mater. Res. Technol. 2019, 8, 1532–1537, doi:10.1016/J.JMRT.2018.08.002.

125. Buyukkaya, E.; Cerit, M. Thermal Analysis of a Ceramic Coating Diesel Engine Piston Using 3-D Finite Element Method. Surf. Coatings Technol. 2007, 202, 398–402, doi:10.1016/J.SURFCOAT.2007.06.006.

126. Sankar, V.; Ramkumar, P.B.; Sebastian, D.; Joseph, D.; Jose, J.; Kurian, A. Optimized Thermal Barrier Coating for Gas Turbine Blades. Mater. Today Proc. 2019, 11, 912–919, doi:10.1016/J.MATPR.2018.12.018.

127. Padture, N.P.; Gell, M.; Jordan, E.H. Thermal Barrier Coatings for Gas-Turbine Engine Applications. Science (80-.). 2002, 296, 280–284, doi:10.1126/SCIENCE.1068609.

128. Clarke, D.R.; Oechsner, M.; Padture, N.P. Thermal-Barrier Coatings for More Efficient Gas-Turbine Engines. MRS Bull. 2012, 37, 891–898, doi:10.1557/MRS.2012.232/FIGURES/8.

129. Ghosh, S.; Saha, M.; Bakshi, S.; Mondal, S. Effect of Thermal Barrier Coating in Sustainable Power Production of Gas Turbines. IOP Conf. Ser. Mater. Sci. Eng. 2021, 1187, 012034, doi:10.1088/1757-899x/1187/1/012034.

130. Jiang, P.; Fan, X.; Sun, Y.; Li, D.; Li, B.; Wang, T. Competition Mechanism of Interfacial Cracks in Thermal Barrier Coating System. Mater. Des. 2017, 132, 559–566, doi:10.1016/J.MATDES.2017.07.018.

131. Naraparaju, R.; Gomez Chavez, J.T.; Schulz, U.; Ramana, C. V. Interaction and Infiltration Behavior of Eyjafjallajökull, Sakurajima Volcanic Ashes and a Synthetic CMAS Containing FeO with/in EB-PVD ZrO2-65 Wt% Y2 O3 Coating at High Temperature. Acta Mater. 2017, 136, 164–180, doi:10.1016/J.ACTAMAT.2017.06.055.

132. Gledhill, A.D.; Reddy, K.M.; Drexler, J.M.; Shinoda, K.; Sampath, S.; Padture, N.P. Mitigation of Damage from Molten Fly Ash to Air-Plasma-Sprayed Thermal Barrier Coatings. Mater. Sci. Eng. A 2011, 528, 7214–7221, doi:10.1016/J.MSEA.2011.06.041.

133. Bonaquist, D.; Feuerstein, A.; Buchakjian, L.; Brooks, P. The Role of Thermal Barrier

135. Grilli, M.L.; Valerini, D.; Slobozeanu, A.E.; Postolnyi, B.O.; Balos, S.; Rizzo, A.; Piticescu, R.R. Critical Raw Materials Saving by Protective Coatings under Extreme Conditions: A Review of Last Trends in Alloys and Coatings for Aerospace Engine Applications. Materials (Basel). 2021, 14, doi:10.3390/MA14071656.

136. Vagge, S.T.; Ghogare, S. Thermal Barrier Coatings: Review. Mater. Today Proc. 2022, 56, 1201–1216, doi:10.1016/J.MATPR.2021.11.170.

137. Urbina, M.; Rinaldi, A.; Cuesta-Lopez, S.; Sobetkii, A.; Slobozeanu, A.E.; Szakalos, P.; Qin, Y.; Prakasam, M.; Piticescu, R.R.; Ducros, C.; et al. The Methodologies and Strategies for the Development of Novel Material Systems and Coatings for Applications in Extreme Environments a Critical Review. Manuf. Rev. 2018, 5, doi:10.1051/MFREVIEW/2018006.

148. Movchan, B.A.; Yu, Y.K. High-Temperature Protective Coatings Produced by EB-PVD. J. Coat. Sci. Technol. 2014, 1, 96–110.

149. Sobetkii, A.; Tudor, A.I.; Rusti, C.F.; Piticescu, R.R.; Rinaldi, A.; Valerini, D. Zirconium Perowskite Coatings Obtained by Combinatorial EB-PVD Process. Proc. - 2018 IEEE Int. Conf. Environ. Electr. Eng. 2018 IEEE Ind. Commer. Power Syst. Eur. EEEIC/I CPS Eur. 2018 2018, doi:10.1109/EEEIC.2018.8494580.

151. Łatka, L. Thermal Barrier Coatings Manufactured by Suspension Plasma Spraying - A Review. Adv. Mater. Sci. 2018, 18, 95–117, doi:10.1515/ADMS-2017-0044.

167. Boissonnet, G.; Chalk, C.; Nicholls, J.R.; Bonnet, G.; Pedraza, F. Phase Stability and Thermal Insulation of YSZ and Erbia-Yttria Co-Doped Zirconia EB-PVD Thermal Barrier Coating Systems. Surf. Coatings Technol. 2020, 389, 125566, doi:10.1016/J.SURFCOAT.2020.125566.

168. Vassen, R.; Cao, X.; Tietz, F.; Basu, D.; Stöver, D. Zirconates as New Materials for Thermal Barrier Coatings. J. Am. Ceram. Soc. 2000, 83, 2023–2028, doi:10.1111/J.1151-2916.2000.TB01506.X.

169. Guo, X.; Li, L.; Park, H.M.; Knapp, J.; Jung, Y.G.; Zhang, J. Mechanical Properties of Layered La2Zr2O7 Thermal Barrier Coatings. J. Therm. Spray Technol. 2018, 27, 581–590, doi:10.1007/S11666-018-0703-5.

170. Zhang, D.; Liao, K.; Yu, Y.; Tian, Z.; Cao, Y. Microstructure and Thermal & Mechanical Properties of La2Zr2O7@YSZ Composite Ceramic. Ceram. Int. 2020, 46, 4737–4747, doi:10.1016/J.CERAMINT.2019.10.205.

171. Karaoglanli, A.C.; Doleker, K.M.; Ozgurluk, Y. Interface Failure Behavior of Yttria Stabilized Zirconia (YSZ), La2Zr2O7, Gd2Zr2O7, YSZ/La2Zr2O7 and YSZ/Gd2Zr2O7 Thermal Barrier Coatings (TBCs) in Thermal Cyclic Exposure. Mater. Charact. 2020, 159, 110072, doi:10.1016/J.MATCHAR.2019.110072.

172. Doleker, K.M.; Ozgurluk, Y.; Karaoglanli, A.C. Isothermal Oxidation and Thermal Cyclic Behaviors of YSZ and Double-Layered YSZ/La2Zr2O7 Thermal Barrier Coatings (TBCs). Surf. Coatings Technol. 2018, 351, 78–88, doi:10.1016/J.SURFCOAT.2018.07.069.

150

173. Naga, S.M.; Awaad, M.; El-Maghraby, H.F.; Hassan, A.M.; Elhoriny, M.; Killinger, A.; Gadow, R. Effect of La2Zr2O7 Coat on the Hot Corrosion of Multi-Layer Thermal Barrier Coatings. Mater. Des. 2016, 102, 1–7, doi:10.1016/J.MATDES.2016.03.133.

174. Wang, C.; Wang, Y.; Fan, S.; You, Y.; Wang, L.; Yang, C.; Sun, X.; Li, X. Optimized Functionally Graded La2Zr2O7/8YSZ Thermal Barrier Coatings Fabricated by Suspension Plasma Spraying. J. Alloys Compd. 2015, 649, 1182–1190, doi:10.1016/J.JALLCOM.2015.05.290.

175. Portinha, A.; Teixeira, V.; Carneiro, J.; Costa, M.F.; Barradas, N.P.; Sequeira, A.D. Stabilization of ZrO2 PVD Coatings with Gd2O3. Surf. Coatings Technol. 2004, 188–189, 107–115, doi:10.1016/J.SURFCOAT.2004.08.016.

176. Cao, X.Q.; Vassen, R.; Jungen, W.; Schwartz, S.; Tietz, F.; Stöver, D. Thermal Stability of Lanthanum Zirconate Plasma-Sprayed Coating. J. Am. Ceram. Soc. 2001, 84, 2086–2090, doi:10.1111/J.1151-2916.2001.TB00962.X.

186. Akram, R.; Natasha; Fahad, S.; Hashmi, M.Z.; Wahid, A.; Adnan, M.; Mubeen, M.; Khan, N.; Rehmani, M.I.A.; Awais, M.; et al. Trends of Electronic Waste Pollution and Its Impact on the Global Environment and Ecosystem. Environ. Sci. Pollut. Res. 2019 2617 2019, 26, 16923–16938, doi:10.1007/S11356-019-04998-2.

187. Gwenzi, W.; Mangori, L.; Danha, C.; Chaukura, N.; Dunjana, N.; Sanganyado, E. Sources, Behaviour, and Environmental and Human Health Risks of High-Technology Rare Earth Elements as Emerging Contaminants. Sci. Total Environ. 2018, 636, 299–313, doi:10.1016/J.SCITOTENV.2018.04.235.

192. Hennig, C.; Weiss, S.; Gumeniuk, R.; Scheinost, A.C. Phase Composition of Yttrium-Doped Zirconia Ceramics. 2017, 2017.

193. Shi, Q.; Yuan, W.; Chao, X.; Zhu, Z. Phase Stability, Thermal Conductivity and Crystal Growth Behavior of RE2O3 (RE = La,Yb,Ce,Gd) Co-Doped Y2O3 Stabilized ZrO2 Powder. J. Sol-Gel Sci. Technol. 2017, 84, 341–348, doi:10.1007/s10971-017-4483-z.

194. Daroonparvar, M.; Yajid, M.A.M.; Yusof, N.M.; Bakhsheshi-Rad, H.R.; Hamzah, E.; Nazoktabar, M. Investigation of Three Steps of Hot Corrosion Process in Y2O3 Stabilized ZrO2 Coatings Including Nano Zones. J. Rare Earths 2014, 32, 989–1002, doi:10.1016/S1002-0721(14)60173-3.

195. Ozgurluk, Y.; Doleker, K.M.; Ozkan, D.; Ahlatci, H.; Karaoglanli, A.C. Cyclic Hot Corrosion Failure Behaviors of EB-PVD TBC Systems in the Presence of Sulfate and Vanadate Molten Salts. Coatings 2019, Vol. 9, Page 166 2019, 9, 166, doi:10.3390/COATINGS9030166.

196. Tao, S.; Yang, J.; Shao, F.; Zhao, H.; Zhong, X.; Zhuang, Y.; Sheng, J.; Ni, J.; Li, Q.; Tao, S. Atmospheric Plasma Sprayed Thick Thermal Barrier Coatings: Microstructure, Thermal Shock Behaviors and Failure Mechanism. Eng. Fail. Anal. 2022, 131, 105819, doi:10.1016/J.ENGFAILANAL.2021.105819.

197. Sun, Y.; Li, J.; Zhang, W.; Wang, T.J. Local Stress Evolution in Thermal Barrier Coating System during Isothermal Growth of Irregular Oxide Layer. Surf. Coatings Technol. 2013, 216, 237–250, doi:10.1016/J.SURFCOAT.2012.11.052.